Expression of GRINA Correlates with Prognosis in Human Cancers: A Pan-cancer Analysis

S. M. Riazul Islam [1, †], Subbroto Kumar Saha [2, 3, †, *], Shaker El-Sappagh [4], Faisal Tariq [5], Joydeep Das [6], Muhammad Afzal [7], and Ssang-Goo Cho [2, *]

[1] Department of Computer Science and Engineering, Sejong University, 209 Neungdong-ro, Gwangjin-gu, Seoul, 05006, Republic of Korea; riaz@sejong.ac.kr (S.M.R.I)

[2] Department of Stem Cell and Regenerative Biotechnology, Konkuk University, 120 Neungdong-Ro, Seoul 05029, Republic of Korea; subbroto@konkuk.ac.kr (S.K.S.).

[3] Department of Biochemistry and Molecular Medicine, University of California at Davis, School of Medicine, Sacramento, California 95817, USA

[4] Centro Singular de Investigación en Tecnoloxías Intelixentes (CiTIUS), Universidade de Santiago de Compostela, 15782, Santiago de Compostela, Spain; shaker.elsappagh@usc.es (S.E.S.)

[5] James Watt School of Engineering, University of Glasgow, Glasgow G12 8QQ, United Kingdom; faisal.tariq@glasgow.ac.uk (F.T.)

[6] School of Chemistry, Shoolini University of Biotechnology and Management Sciences, Bajhol, Sultanpur, Solan – 173229 (HP), India; jdchem83@gmail.com (J.D.)

[7] Department of Software, Sejong University, Seoul 05006, South Korea; mafzal@sejong.ac.kr (M.A.)

[†] These authors contributed equally to this work: S.M.R. Islam and S.K. Saha (co-first authors)

[*] Correspondence: sksaha@ucdavis.edu (S.K.S.); ssangoo@konkuk.ac.kr (S.-G.C.); Tel.: +1 (410) 413-0532 (S.K.S.); Tel.: +82-2-450-4207 (S.-G.C.); Fax: +82-2-444-4207 (S.-G.C.)

Abstract: *GRINA* is an emerging target for cancer therapy. However, the role of *GRINA* expression and its correlation with cancer patient survival has not been comprehensively studied. Here, we found that mRNA and protein expression of GRINA was upregulated in breast, colon, gastric, and prostate cancers and negatively correlated with patient survival. Also, the upregulation of GRINA expression is associated with hypomethylation of its promoter region. Our GRINA-miRNAs network analysis revealed potential regulatory miRNAs regulating the GRINA expression and its downstream pathways. Next, functional enrichment and pathway analysis of genes commonly co-express with *GRINA* in breast, colon, gastric, and prostate cancers revealed *GRINA* regulatory pathways. Concurrently, our upstream regulator analysis revealed possible kinases, transcription factors, and proteins that may potentially regulate *GRINA* . Overall, this study demonstrates the prognostic significance of *GRINA* expression and identifies potential regulatory mechanisms, which might have significant implications in targeted therapies for human cancers.

Keywords: glutamate receptor; GRINA; cancer biomarker; multiomics; cancer survival

1. Introduction

Targeted therapy is an emerging paradigm in molecular medicine for next-generation cancer treatment. Recently, targeting the N-methyl-D-aspartate (NMDA) receptor expressed on the surfaces of cancer cells has emerged as a therapeutic approach [1]. NMDA receptors regulate the mammalian target of rapamycin (mTOR), a kinase involved in signaling that is a therapeutic target for many types of cancers [2-4]. Triggering the inappropriate expression of NMDA receptors on cancer cell lines thus represents a possible therapeutic avenue to control dysregulated cancer cell growth, division, and invasiveness [5, 6]. For example, NMDA receptors have been closely associated with tumor progression [7]. Inactivation of NMDA receptors in breast and lung cancers can potentially trigger apoptosis of tumor cells, and the NMDA receptor is a prospective therapeutic marker for ovarian cancer [8]. Also, NMDA2B phosphorylation can inhibit epileptic seizures triggered by brain tumors [9]. An essential constituent of NMDA heteromers in the NR2A subunit, the loss of which in gastric cancers can cause cell cycle arrest and prevent the proliferation of MKN45 [10].

One of the most common receptors belonging to the NMDA receptor family is GRINA, also known as transmembrane BAX inhibitor motif-containing (TMBIM3). GRINA, like other TMBIM members, is a regulator of cell death. All TMBIM family members inhibit different aspects of apoptosis, including ER modulation, calcium homeostasis, and ER stress signaling [11]. ER stress has also been shown to trigger TMBIM3/*GRINA* expression in defense against ER stress-triggered apoptosis [12]. GRINA also plays significant roles in cell proliferation, invasion, and migration [13], is strongly expressed in the central nervous

system [14], and is overexpressed in breast cancer tissue [15]. Besides, *GRINA* mRNA is significantly upregulated in the prefrontal cortex of human subjects with a depressive disorder [16]. These findings suggest that GRINA may play a significant role in the progression of multiple cancers.

The existence of the volume of research on TMBIM members and their dysregulation in various cancer types [17-19] implies that the *GRINA* gene could be useful in finding innovative approaches for specific cancer therapies. *GRINA* mRNA levels as diagnostic markers in cancers can be considered an emerging area of research [11, 13, 14]. However, to the best of our knowledge, this gene has not been studied from a data mining perspective yet. In this study, we use multi-omics analysis to systematically evaluate the biomarker importance and prognostic significance of *GRINA* for multiple cancers. *GRINA* expression patterns and clinical outcomes of certain cancers were compared using expression, function, and patient survival datasets accessible online. We also investigated several regulatory mechanisms that may underlie *GRINA* function in our cancers of interest by probing for miRNA-mRNA interactions, co-expressed proteins, pathway activity, and interactions between kinases and transcription factors. This bioinformatics analysis ultimately demonstrated that *GRINA* expression could be used as a biomarker for determining prognoses for patients with certain types of cancers.

2. Experimental Section

2.1. GRINA mRNA and Protein Expression, Promoter Methylation, and Copy Number Alterations (CNAs) Analysis

The Oncomine platform (https://www.oncomine.org/resource/login.html) was used to analyze and visualize the *GRINA* mRNA expression [20-23]. Default threshold parameters were selected, consisting of *p*-value = 1E-4, fold-change = 2, and gene ranking in the top 10%. Statistical analyses were performed using an unpaired *t*-test, and $p < 0.05$ was considered significant.

GRINA mRNA expression in various types of cancer and normal tissues was examined using TCGA level 3 RNA-seq datasets via UCSC Xena (https://xenabrowser.net/heatmap/) [24]. Statistical analyses were performed using a Welch's t-test, and $p < 0.05$ was considered significant.

GRINA mRNA expression in subclasses of multiple cancers, including breast, colon, gastric, and prostate cancers, was also determined using TCGA level 3 RNA-seq datasets via ULCAN (http://ualcan.path.uab.edu/index.html) [25]. Methylation values of *GRINA* gene promoter in cancers, such as breast, colon, gastric, and prostate cancer, were examined using TCGA datasets via ULCAN. Statistical analyses were performed using a student's t-test, and $p < 0.05$ was considered significant.

GRINA mRNA expression in various cancer cell lines was analyzed by RT-PCR. For RT-PCR analysis, total RNA was extracted from used cell lines using the Easy-Blue RNA Extraction kit (iNtRON Biotechnology, Seongnam-si, Gyeonggi-do, Korea). According to the manufacturer's instructions, total RNA (2 μg) was reverse transcribed into cDNA using a cDNA synthesis kit (Promega, Madison, WI, USA). The RT-PCR was assessed using r-Taq plus Master Mix (Elpis Biotech, Daejeon, Korea), and the PCR products were analyzed by

~1.5% agarose gel electrophoresis. The bands were separated in agarose gels containing ethidium bromide (EtBr) and observed under UV light. The pictures were analyzed in Photoshop CS6 (Version 13.0.6 x64, San Jose, CA, USA), and the relative expression fold changes were measured in ImageJ [26]. The primers were used as Forward primer 5'-ATTCTCTGCATCTTCATCCGG-3'; Reverse primer 5'-AAACACATACTCTTCTGGGCTC-3' for *GRINA* and Forward primer 5'-AATCCCATCACCATCTTCCAG-3'; Reverse primer 5'-CACGATACCAAAGTTGTCATGG-3' for *GAPDH*.

GRINA protein expression in cancerous and normal tissues was examined using immunohistochemistry (IHC) staining data from the Human Protein Atlas (https://www.proteinatlas.org/) [27, 28]. For IHC staining, the HPA036980 antibody targeting GRINA was used.

Copy number alterations (CNAs) of *GRINA* in various types of cancer were examined using TCGA datasets via cBioPortal (https://www.cbioportal.org/) [29, 30].

2.2. Prognosis Analysis Using R2: Kaplan Meier Scanner (Pro) and SurvExpress

The prognostic relationship between *GRINA* levels and cancer patient survival was investigated using the R2: Kaplan Meier Scanner web (https://hgserver1.amc.nl/cgi-bin/r2/main.cgi) [31] and using SurvExpress web (http://bioinformatica.mty.itesm.mx:8080/Biomatec/SurvivaX.jsp) [32]. Survival curve

131 analysis was conducted using a threshold log-rank test using scan modus of expression value.
132 Statistical significance was indicated by $p < 0.05$.

133 2.3. Construction of the GRINA-miRNA-mRNA Regulatory Network

134 miRNAs targeting *GRINA* mRNA were predicted and retrieved from miRSystem
135 (http://mirsystem.cgm.ntu.edu.tw/index.php) [33] and starBase v3.0
136 (http://starbase.sysu.edu.cn/)[34]. Retrieved miRNAs were visualized as a Venn diagram
137 using Venny v1.2 (https://bioinfogp.cnb.csic.es/tools/venny/) [35]. The *GRINA*-miRNA-
138 mRNA regulatory network was constructed using starBase v3.0 to identify potential *GRINA*-
139 binding miRNAs. Expression levels of these miRNAs in breast cancer were also determined
140 using starBase v3.0 (http://starbase.sysu.edu.cn/). A Student's t-test was performed to
141 generate a *p*-value, which indicates the significance of an observation. $p < 0.05$ was
142 considered statistically significant. The binding site of GRINA 3'UTR and miRNAs were
143 derived from Starbase v3.0 web.

144 2.4. Gene Ontology (GO) and Pathway Analysis of GRINA Co-expressed Genes

145 Genes positively and negatively co-expressed with *GRINA* in selected cancers were
146 retrieved from the TCGA data using R2: Genomics Analysis and Visualization Platform
147 (https://hgserver1.amc.nl/cgi-bin/r2/main.cgi?&species=hs) [31]. Positively and negatively
148 co-expressed genes were considered as those with r value -0.30 > and > 0.30 and $P \leq 0.01$.
149 Genes showing co-expression with *GRINA* in breast, colon, stomach, and prostate cancers
150 were assembled into a Venn diagram via InteractiVenn

(http://www.interactivenn.net/index.html) to identify the common positively and negatively co-expressed genes of GRINA [36]. The common genes co-expressed with *GRINA* in breast, colon, stomach, and prostate cancers were then used to analyze gene ontology and pathway enrichment using Enrichr (https://amp.pharm.mssm.edu/Enrichr/) [37, 38]. The bar graphs retrieved from Enrichr web were ranked by *p*-value from several databases, including the Kyoto Encyclopedia of Genes and Genomes (KEGG)-2019, Reactome pathway-2016, and GO (biological process, molecular function, and cellular component)-2018.

2.5. Transcription Factors and Protein Kinases Associated with Genes Co-expressed with GRINA

Upstream regulators and protein kinases associated with genes co-expressed with *GRINA* were identified by submitting the list of co-expressed genes to Expression2Kinases (X2K) web interface (https://amp.pharm.mssm.edu/X2K/) [39, 40], which identifies enriched transcription factors (TFs) upstream of the co-expressed genes using the ChEA database. Genes2Networks (G2N) module of X2K connected TFs with protein-protein interaction to identify transcriptional complexes related to these gene signatures. Protein kinases responsible for TF complex formation and regulation were recognized through the Kinase Enrichment Analysis (KEA) module of X2K. The top 10 most enriched TFs and kinases were ranked based on a combined P-value and z-score value.

To have a quick review of the aforementioned online tools, we have presented a schematic diagram that summarizes their functions in Figure 1.

3. Results

3.1. GRINA mRNA Expression in Various Cancers

To examine *GRINA* mRNA expression levels in select normal and cancer types tissues, we utilized online analytical tools and databases, including Oncomine and TCGA. A significant number of analyses performed using the Oncomine platform revealed high *GRINA* expression in breast, colon, gastric, lymphoma, melanoma, ovarian, and prostate cancers (Figure 2a; Supplementary Table 1). The Oncomine platform also indicated the downregulation of *GRINA* in oesophageal, head-and-neck, and lung cancers (Figure 2a; Supplementary Table 1). To confirm the relative levels of *GRINA* expression in normal and cancerous tissues, we further analyzed expression data using the TCGA data-driven UCSC Xena online tool, which yielded similar results to those from Oncomine-based analysis (Figure 2b; Supplementary Table 2). We further experimentally confirmed the expression pattern of *GRINA* in various cancer cell lines using RT-PCR analysis (Figure 2c). According to the experimental outcomes, the mRNA expression of *GRINA* was upregulated in the breast (MCF7 and MDA-MB231 cell lines), colon (HCT116 and HT-29 cell lines), blood (K562 cell line), and ovarian (SKOV3 and A2780 cell lines). At the same time, it was comparatively downregulated in the esophagus (SEG-1 cell line), liver (HepG2 and SNU475 cell lines), and lung (A549 cell line) cancer. In summary, analysis with Oncomine and TCGA databases commonly showed *GRINA* overexpression in multiple cancers. Therefore, based on high *GRINA* expression levels, we selected breast, colon, gastric, and prostate cancers for further systematic analysis of *GRINA* expression and its clinical significance. It is worth noting that we used Oncomine and TCGA databases to present the expression status of *GRINA* in various

cancers. The primary purpose of this expression checking was to find the four most common cancers in terms of high *GRINA* expression. It can be noted that our purpose of the multi-omics analysis is not to see the *GRINA* expression status individually. Instead, we used multi-omics analysis to show consistencies between *GRINA* expression and other genetic statuses such as methylation of *GRINA* promoters, mutation and CNA, and immunostaining results, as will be analyzed subsequently.

3.2. GRINA Expression Patterns and Patient Survival of Breast Cancer

To investigate *GRINA* expression in breast cancer and corresponding normal tissue samples, we evaluated Oncomine and TCGA datasets. Relative expression levels of *GRINA* in 21 lobular breast cancer (LBC) and 38 invasive ductal breast cancer (IDBC) tissues were analyzed in the Zhao dataset. Compared to histologically normal breast tissue (n = 3) derived from IDBC patients used in the Zhao dataset, *GRINA* is significantly overexpressed in both LBC and IDBC tissues (Figure 3a-b). In addition, *GRINA* mRNA levels are significantly (p < 1.63E-12) higher in invasive breast carcinoma (BRIC) tissue than normal tissue (Figure 3c) based on the analysis of 114 normal breast tissue samples and 1097 breast cancer tissue samples from the TCGA-driven ULCAN dataset. To analyze GRINA expression and patient subclass associations, we determined *GRINA* levels in normal, luminal, human epidermal growth factor receptor 2 positive (HER2+), and triple-negative breast cancer positive (TNBC+) groups, which were derived from 833 patient samples in the TCGA dataset using ULCAN. *GRINA* mRNA levels are significantly higher in luminal (p = 1.63E−12), HER2+ (p = 2.22E−5), and TNBC+ (p = 3.86E−6) subclasses (Figure 3d). In addition, the average

methylation level of *GRINA* gene promoters in breast cancer samples is significantly lower compared to that in normal breast samples (Figure 3e). A lack of methylation of *GRINA* promoters in breast cancer may thus cause *GRINA* upregulation of this gene. We next analyzed mutation and copy number alteration (CNA) of *GRINA* in breast cancer using cBioPortal. Alterations of the *GRINA* gene, including amplification and deep deletion, were found in 32% of 1088 cases (Figure 3f). *GRINA* mRNA levels were high in approximately 50% of altered samples, suggesting that *GRINA* expression in breast cancer is positively correlated with CNA status. Such amplification likely underlies increases in *GRINA* expression.

Protein expression patterns of GRINA in breast cancer were examined using immunohistochemical (IHC) staining and the Human Protein Atlas. These results confirm the overexpression of *GRINA* at the protein levels in breast cancer samples relative to normal breast tissue (Figure 3g). In addition, we investigated the relationship between *GRINA* expression and clinical prognosis using the R2: Kaplan Meier Scanner. Patients with high levels of *GRINA* (n = 42) had significantly (p = 9.1E-06) lower overall survival compared to patients with lower *GRINA* levels (n = 1054) (Figure 3h). *GRINA* levels are thus significantly augmented in breast cancer cells and positively correlated with poor patient prognosis.

3.3. GRINA Expression Patterns and Patient Survival of Colon Cancer

We next examined *GRINA* characteristics in colon cancer (Figure 2a-d). Upregulation patterns of *GRINA* in colon cancer have previously been reported [11, 41]; however, the

correlation between *GRINA* expression and patient prognosis has not been systematically analyzed. We thus evaluated *GRINA* expression in microarray datasets for colon cancer and normal tissues using Oncomine. In addition, relative expression levels of *GRINA* in colon carcinomas (CC) and 65 rectal adenocarcinomas were analyzed using the Skrzypczak and Gaedcke datasets. Compared to normal colon tissue, *GRINA* was significantly upregulated in both cases (Figures 4a and b). We also analyzed *GRINA* levels in 41 colon normal tissue samples and 286 colon cancer tissue samples. As observed for breast cancer samples, *GRINA* expression was significantly ($p < 1E{-}12$) augmented in colon adenocarcinomas (COAD) compared to normal tissues (Figure 4c).

We also analyzed 321 patient samples in the TCGA dataset to examine the relationship between *GRINA* expression and colon cancer patient subclass. GRINA mRNA levels were significantly elevated in COAD ($p = 1.63E{-}{-}12$) and mucinous-adenocarcinoma (MADC) ($p = 8.09E{-}10$) subclasses (Figure 4d), which is supported by the hypomethylation of the GRINA gene promoter in colon cancer specimens. However, the difference between normal and cancer is not statistically significant (Figure 4e). In addition, mutation and CNA analysis of *GRINA* in colon cancer samples using cBioPortal revealed that *GRINA* levels positively correlated with CNA status, as 85 out of 117 colon cancer cases with altered samples showed high *GRINA* mRNA levels (Figure 4f). While amplification occurred in a handful of cases, no specific mutation appeared to cause *GRINA* alterations.

We also examined GRINA protein expression in colon cancer specimens using IHC staining information from the human protein atlas web. As presented in Figure 4g, GRINA

overexpression was visible across the entire colon cancer tissue sample compared to normal tissue. We then analyzed colon cancer patients' clinical outcomes to understand the relationship between prognosis and *GRINA* expression. The R2: Kaplan Meier Scanner was applied to data from 147 patients with high *GRINA* expression and 79 patients with low *GRINA* expression. Patients with high *GRINA* levels experienced poorer relapse-free survival (Figure 4h). Thus, these results suggest that high GRINA expression due to copy number alterations are common in colon cancer tissue and positively correlates with low patient survival.

3.4. GRINA Expression Patterns and Patient Survival in Gastric Cancer

We also examined *GRINA* levels in gastric carcinoma (GC) in which *GRINA* overexpression has previously been observed [13, 42, 43]. We thus performed a systematic analysis to evaluate the association between *GRINA* expression and clinical outcomes of gastric cancer patients. Relative *GRINA* mRNA levels in 26 Gastric Intestinal Type Adenocarcinoma (GITA) and 4 Gastric Mixed Adenocarcinoma (GMA) were analyzed based on the DErrico datasets using the Oncomine platform. *GRINA* levels are significantly altered in both types of gastric cancers compared to normal gastric tissue (Figure 5a and b). Analysis of *GRINA* expression in a larger TCGA dataset consisting of 34 normal stomach tissue samples and 415 gastric cancer tissue samples confirmed expression patterns described above, as *GRINA* was significantly ($p < 1.63E{-}12$) overexpressed in gastric cancer samples (Figure 5c). Next, TCGA was used to access data from 440 patients and determine whether it was possible to differentiate between gastric cancer grades based on *GRINA* levels. While

GRINA mRNA levels were significantly elevated in each gastric cancer grade (Figure 5d), expression levels alone did not always indicate the cancer stage, as Grade 3 gastric cancers exhibited the lowest levels of *GRINA*.

To evaluate the consistency in *GRINA* levels with *GRINA* promoter methylation, we compared the beta values of *GRINA* promoter methylation in normal gastric and cancerous gastric tissues. A large but non-significant difference in beta values between gastric cancer and normal samples was observed (Figure 5e), suggesting elevated *GRINA* mRNA levels in gastric cancer. Out of these altered cases, 64% (63 out of 98 altered cases) showed high *GRINA* mRNA levels (Figure 5f), indicating a positive association between CNA status and *GRINA* levels in gastric cancer. IHC results with gastric cancer specimens also decisively indicate increased *GRINA* din gastric cancer (Figure 5g). We next investigated whether *GRINA* expression likely relates to gastric cancer prognosis. Using the same number of patients as in the colon cancer analysis, R2: Kaplan Meier Scanner analysis of gastric cancer cases indicated an association between poor overall patient survival and higher *GRINA* mRNA levels (Figure 5h). Taken together, *GRINA* overexpression is expected in most gastric cancer cases and positively associates with poor clinical prognosis.

3.5. GRINA Expression Patterns and Patient Survival of Prostate Cancer

GRINA mRNA expression is known to be highly upregulated in prostate cancer tissues compared to normal tissues based on online tools and databases (Figure 6a-d). Our detailed analysis showed that elevated *GRINA* expression was evident in prostate carcinomas and

prostatic intraepithelial neoplasias based on Oncomine (Figure 6a and b) using the Tomlins datasets. *GRINA* expression was also significantly (p = 4.82E-14) upregulated in prostate adenocarcinomas (PRAD) according to analysis using the TCGA database (Figure 6c) and considering 52 normal prostate tissue samples and 497 prostate cancer tissue samples. For prostate cancer, *GRINA* mRNA expression patterns can be translated into Gleason scores (GS), which range from 1 to 5, and describe whether prostate tissue biopsies resemble normal tissues (lower score) or abnormal tissues (higher score). As presented in Figure 6d, *GRINA* levels and the GS exhibited linear relationships, indicating that the most melancholy GRINA expression in prostate cancer represents GS 1. The highest *GRINA* levels represent GS 5, and *GRINA* levels corresponding to other GS values can be determined using a simple linear transformation.

Methylation status analysis revealed that the *GRINA* gene promoter was significantly hypomethylated in prostate cancer tissues, confirming mRNA overexpression patterns of *GRINA* (Figure 6e). In addition, CNA status and *GRINA* expression levels in prostate cancer were positively correlated, with ~ 67% (60 out of 89 altered cases) of altered samples showing high levels of *GRINA* mRNA (Figure 6f). Human Protein Atlas-assisted immunostaining confirmed the GRINA protein overexpression in prostate cancer samples compared to normal samples (Figure 6g). Finally, we investigated the prognostic significance of *GRINA* expression levels for prostate cancer. R2: Kaplan Meier Scanner survival analysis of data for a set of 247 patients with high *GRINA* levels and 250 patients with low *GRINA* levels revealed that prostate cancer patients with high *GRINA* levels showed significantly

poorer overall survival compared to the low *GRINA* expression patients (Figure 6h). Overall, the available data demonstrated altered expression levels of *GRINA* in prostate cancer and their associated prognostic utility.

3.6. GRINA Expression Patterns and Patient Survival for Additional Cancer Types

Although the primary focus of this study was to understand *GRINA* expression levels and their clinical significance in the four cancers presented above, we also analyzed *GRINA* expression levels and their relevance to clinical outcomes in other cancers. Based on Oncomine analyses, *GRINA* expression was elevated in cancers such as lymphoma, melanoma, ovarian, and sarcoma cancers (Figure 2b). Using TCGA database-enabled ULCAN analysis, significant upregulation of *GRINA* was found in many additional cancers, including bladder, cholangial, oesophageal, head-and-neck, liver, rectum, and uterine cancers (Supplementary Figure 2). Our analysis did not identify any cancers in which *GRINA* was significantly ($p < 0.05$) downregulated. To understand the prognostic relevance of *GRINA* levels, analysis of survival rates and *GRINA* levels was performed using the SurvExpress platform based on TCGA data. This analysis showed that *GRINA* levels positively correlated with low patient survival in cancers such as the bladder, cholangial, and rectum cancers but not uterine cancer, as indicated by hazard ratios (Supplementary Figure 3). These findings suggested that *GRINA* levels are probably associated with biological mechanisms that promote aggressiveness to some extent in most cancers.

3.7. Analysis of Potential GRINA-miRNA-mRNA Regulatory Networks

After analyzing *GRINA* expression patterns and clinical relevance in various cancer types, we focused on a couple of underlying regulatory mechanisms of *GRINA* in our cancers of interest. Several studies [44, 45] suggest that microRNA (miRNA)-targeting genes can be utilized as prognostic predictors for individual cancer patients, conforming to the competing endogenous RNA (ceRNAs) hypothesis. We thus built and analyzed a potential *GRINA*-miRNA-mRNA regulatory network. Using the miRSystem, 41 miRNAs were found that potentially targeted *GRINA*, while starBase provided 54 such miRNAs (Figure 7a). A total of 18 of these miRNAs appeared on both platforms. It was chosen as candidate miRNAs for targeting *GRINA* mRNA to use with the starBase web to create a *GRINA*-miRNA-mRNA regulatory network (Figure 7b). As shown earlier, *GRINA* is upregulated in breast, colon, gastric, and prostate cancers. To conform with these mRNA expression patterns, expression levels of *GRINA*-targeting miRNAs should be lower in cancers compared to normal controls, according to the ceRNA model. We, therefore, examined expression levels of the 18 potential *GRINA*-targeting miRNAs in the aforementioned cancers. miR-411-5p, miR-654-5p, and miR-874-3p were marked as representative miRNAs because the expression levels of these miRNAs are significantly lower in cancerous tissues than other miRNAs. miRNA expression patterns of miR-411-5p, miR-654-5p, and miR-874-3p in the above cancers followed the ceRNAs mechanism, except for miR-411-5p in colon cancer and both miR-654-5p and miR-874-3p in gastric cancer (Figure 7c). In silico algorithms (Starbase v3.0) were also utilized to identify the binding sites of predicted miRNAs (miR-411, miR-654, and miR-874) that targeted the 3′ UTR region of the GRINA gene. The results showed that our predicted

358 miRNAs were explicitly bound to the 3'UTR region of the GRINA gene, implying direct
359 prevention of GRINA transcription via miR-411, miR-654, and miR-874 (Figure 7d (i-iii)).
360 Our findings suggest that *GRINA* may have oncogenic roles in breast and prostate cancers
361 via this miRNA-mRNA regulatory network. However, other unknown factors could
362 overshadow the roles of the miRNA-mRNA network on the oncogenic behavior of *GRINA*
363 in the colon and gastric cancers.

364 3.8. Identification and Functional Enrichment Analysis of Genes Co-expressed with GRINA

365 To understand how *GRINA* functions in conjunction with other genes in signaling
366 pathways in breast, colon, gastric, and prostate cancers, co-expression with *GRINA* was
367 analyzed using TCGA data through the R2: Genomics Analysis and Visualization Platform.
368 Eighty-three genes were upregulated with *GRINA* upregulation ("Positive Cluster") (Figure
369 8a), while 21 genes were downregulated with *GRINA* upregulation ("Negative Cluster")
370 (Figure 8d). To understand the function of these genes, gene ontology (GO) functional
371 annotation and pathway enrichment analysis were performed using the Enrichr platform.
372 Three GO functional annotation categories for each cluster were obtained: biological process,
373 cellular component, and molecular function. For the positive cluster, attachment of GPI
374 (glycosylphosphatidylinositol) anchor to protein, GPI anchor binding, and mRNA cleavage
375 and polyadenylation specificity factor complex were the most significantly represented GO
376 terms in the biological process, cellular component, and molecular function, respectively
377 (Supplementary Figure 4a-c). Conversely, entirely different sets of ontologies were
378 associated with the negatively co-expressed gene cluster. The most prominent cellular

component is mutLapha complex, with several critical biological processes including DNA binding, siRNA binding, and helicase activity and molecular functions related to this cluster (Supplementary Figure 4d-f).

We performed Reactome and KEGG (Kyoto Encyclopedia of Genes and Genomes) pathway analysis for both the positive and negative clusters. Our Reactome pathway analysis revealed that some positive cluster genes were associated with pathways related to cell surface events, including insulin receptor recycling, transferrin endocytosis and recycling, and attachment of GPI anchors to uPAR (Figure 8b). Some categories involved post-transcriptional protein regulation, such as the synthesis of GPI-anchored proteins. For negative cluster genes, pathways related to the cell cycle and transcriptional regulation, such as cell cycle, gene expression, and gene silencing by RNA, predominated (Figure 8e). KEGG analysis indicated that glycosylphosphatidylinositol (GPI)-anchor biosynthesis, which was also found in Reactome pathway analysis, was the prominent pathway for the positive cluster (Figure 8c). In addition, KEGG analysis indicated that some negative cluster genes were associated with p53 signaling, apoptosis, and RNA transport (Figure 8f). Thus, our findings suggested that the biological pathways involved in regulating genes positively co-expressed with GRINA are fundamentally different from those showing negative co-expression with GRINA. GRINA may be associated with specific critical pathways related to cell surface dynamics and post-transcriptional control in cancer development.

3.9. Upstream Regulator Analysis of Genes Co-expressed with GRINA

We also identified transcription factors, intermediate proteins, and associated protein kinases potentially related to regulating co-expression of genes with *GRINA* using the Expression2Kinases (X2K) platform. X2K analysis revealed that PML, HNF4A, and TAF1 are major transcription factors that bind to positive cluster genes (Figure 9a; Supplementary Table 3), whereas STAT3, PPARG, and EGR1 are prominent transcription factors associated with negative cluster genes (Figure 9b; Supplementary Table 3). Transcription factors associated with upregulated genes were generally distinct from those associated with downregulated genes except for TAF1.

We also noticed that these transcription factors of interest for both the positive and negative clusters related to a large number of intermediate proteins that may assist with transcription factor activation. In addition, protein kinases such as MAPK14, ATM, and CK2ALPHA for positively co-expressed genes (Figure 9a; Supplementary Table 4) and GK3B, MAPK14, and MAPK3 for negatively co-expressed genes (Figure 9b; Supplementary Table 4) showed connections with many intermediate proteins associated with transcription factors belonging to each cluster. The only protein kinase in common between the positive and negative clusters was MAPK14. Promyelocytic leukemia protein (PML) and signal transducer and activator of transcription 3 (STAT3) showed the largest numbers of direct/indirect connections. They were labeled hub proteins of the positive and negative cluster genes, respectively. Our findings suggest that candidate hub proteins and their downstream targets may play significant roles in the progression of breast, colon, gastric, and

prostate cancers. These transcription factors thus can be considered potential biomarkers and may be utilized in targeted therapy for the above cancers.

4. Discussion

GRINA belongs to the TMBIM protein family and is involved in calcium homeostasis, regulating various vital processes such as cell survival and neurotransmitter release. Alterations in the roles of *GRINA* are associated with schizophrenia and celiac disease [41]. Irregular *GRINA* expression patterns are found in several cancers, and elevated *GRINA* levels promote gastric cancer growth [13]. In contrast, *GRINA* is downregulated in the post-mortem superior temporal gyrus of schizophrenia patients [46]. Although its relevance is still unknown, alternative splicing of *GRINA* is found in the cortex of Alzheimer's patients and cutaneous horn cancer [47]. GRINA is one of the most common NMDA receptors. NMDA receptors' expressions were reported in human ovarian cancer tissues and human ovarian cancer cell lines [8]. As they were expressed in breast cancer and small-cell lung cancer, these receptors can potentially be targeted to trigger cancer cell death [3, 4]. Overexcitation of the extrasynaptic receptors in the peritumoral neurons was linked to the development of peritumoral seizures [48]. GRINA is also predominantly expressed in the brain [49]. In our current study, we analyzed *GRINA* expression in various cancers using bioinformatics tools and multiple gene expression datasets. Our analysis showed that *GRINA* expression is significantly elevated in multiple cancer cells compared to their normal counterparts. The consistency of *GRINA* expression patterns in each cancer of interest was crosschecked using different databases and confirmed based on *GRINA* promoter and immunostaining results.

GRINA mRNA levels positively correlated with alteration frequency and negatively correlated with patient survival in breast, colon, gastric, and prostate cancers. These results suggest that *GRINA* function significantly affects the prognosis and progression of various cancers. In addition, the consistent elevation of *GRINA* expression in cancers indicates some commonality amongst different cancer types where *GRINA*-centric regulatory mechanisms may function. As *GRINA* expression is variable and has a wide range in many tumors, the question then comes to interpreting this variability in the clinical setting. In molecular therapeutic target viewpoint, the elevated expression of *GRINA* in the cancer of interest first conveys biomarker significance. Because of the confirmed augmented expression, the physician might be more confident to apply the targeted therapies. Then, the strength to which these targeted drugs should be clinically applied does partly come from GRINA expression variability. However, adequate prior clinical trials must be conducted to see whether they can be approved for broader use. The existence of co-expressed genes with *GRINA* can appear as additional confirmation of the biomarker role of *GRINA* and the strength of the *GRINA*-mediated targeted therapies.

To reveal potential *GRINA*-related molecular mechanisms and signaling pathways, we examined *GRINA* miRNA-mRNA regulatory networks, the identities and function of genes co-expressed with *GRINA*, and upstream regulator analysis of those co-expressed genes. Analysis of miRNA-mediated post-transcriptional regulation of *GRINA* mRNAs identified miR-411-5p, miR-654-5p, and miR-874-3p as miRNAs of interest, the expression of which was significantly lower in breast and prostate cancers, following the ceRNA model.

Relatively low expression levels of these miRNAs were also noticed in the colon and gastric, with some minor exceptions. There exist some evidence that miRNA post-transcriptionally regulates *GRINA* expression at both mRNA and protein levels. A study reported that several microRNAs such as miR-411 were predicted to target alcohol-responsive mRNAs, including *GRINA* [50].

Interestingly, miR-411 is also found in our miRNA-mRNA analysis. *GRINA* was also significantly upregulated in human trabecular meshwork cells after overexpression of miR-24 mimic [51]. Moreover, *GRINA* has an important activity controlling cell death induced by ER stress suggesting a functional interconnection between *GRINA* and its role in the control of cell death and ER calcium homeostasis [52]. Our analysis indicates that a regulatory network consisting of miRNAs, including miR-411-5p, miR-654-5p, and miR-874-3p, may facilitate the oncogenic roles of *GRINA* in certain cancers.

Co-expression analysis may also provide important information for investigating mechanisms of *GRINA* function. A positive correlation between the expression of several genes and *GRINA* levels was observed in breast, colon, gastric, and prostate cancers, 83 of which occurred in all cancers. In contrast, the number of negatively co-expressed genes present in all cancers examined was 21. Functional enrichment analysis of positively co-expressed genes revealed that GPI anchor to protein, GPI anchor binding, and mRNA cleavage and polyadenylation specificity factor complex were the most significantly enriched GO terms. Reactome pathway analysis showed that insulin receptor recycling, transferrin endocytosis and recycling, attachment of GPI anchor to uPAR, and post-translational

482 modification and synthesis of GPI-anchored proteins were the major pathways associated
483 with the positively co-expressed genes. Cell surface dynamics and post-transcriptional
484 modification of *GRINA* have also been previously reported [41, 53, 54]. Noticeably, GO
485 terms and pathways related to genes negatively co-expressed with *GRINA* were completely
486 different from those related to positively co-expressed genes. Our findings suggest that
487 pathways involving cell surface dynamics and post-transcriptional regulation may underpin
488 the role of *GRINA* in cancer.

489 We next performed upstream regulator analysis of genes co-expressed with *GRINA* to
490 identify associated major transcription factors. This analysis revealed that transcription
491 factors regulating positive and negative cluster genes were influenced by many intermediate
492 proteins modulated by specific kinases. The major transcription factors binding to positive
493 cluster genes were PML, HNF4A, and TAF1, while major transcription factors associated
494 with negative cluster genes were STAT3, PPARG, and EGR1. In addition, PML and STAT3
495 acted as hub proteins of the positively correlated genes and negatively correlated genes,
496 respectively. The roles of PML and STAT3 as hub proteins in the said cancers are also
497 evident from previous research. For example, the study showed that PML promotes
498 metastasis of TNBC [55], and targeting PML elicits its growth suppression [56]. Also, the
499 expression level of PML is the potential to predict prostate cancer progression [57] and
500 gastric cancer [58]. Furthermore, histochemical analyses of clinical samples have shown
501 PML to be downregulated in colon cancer [59]. On the other hand, STAT3 might serve as a
502 therapeutic target for various cancers such as gastric [60] and TNBC [61]. Our findings thus

503 indicate that the PML could be used as a biomarker in *GRINA*-mediated targeted therapy for
504 breast, colon, gastric, and prostate cancers.

505 In this study, we investigated the expression, methylation, genetic alteration, and
506 immunostaining patterns of *GRINA*. We evaluated its prognostic use through organized data
507 analysis using several established bioinformatics tools, with expression and clinical data
508 obtained from various open-source platforms. Our study showed that the expression,
509 methylation, and immunostaining of *GRINA* collectively convey biomarker significance for
510 breast, colon, gastric, and prostate cancers, among others. The overexpression of *GRINA* was
511 in agreement with its promoter methylation level in the aforementioned cancers. However,
512 the results of hypomethylation of the *GRINA* gene promoter in breast and prostate cancers
513 were more significant compared to that in colon and gastric cancers. Our analysis also
514 indicates that high *GRINA* expression positively correlates with poor prognosis in patients
515 with the said cancers. The silico data mining of miRNA reveals that the regulatory network
516 containing miR-411-5p, miR-654-5p, and miR-874-3p may contributes to the oncogenic
517 roles of *GRINA* to some extent. In sum, this study tried to gain some insights into the
518 oncogenic roles of *GRINA* by revealing the respective miRNA-mRNA interactions, genes
519 co-expressed with *GRINA* and their associated pathways, and specific kinases, transcription
520 factors, and accompanying intermediate proteins that could collectively underpin the
521 regulation of *GRINA* expression. However, it is worth to note that data mining only
522 constitutes the first step of a scientific investigation. Since there is no prominent and useful
523 study and review on GRINA with data analysis perspective, we thus became motivated to

524 investigate the expression and related molecular mechanisms of the GRINA gene and find
525 their relevance to prognostic significance through systematic data analysis using publicly
526 available expression and clinical outcomes data. On that, further research is required to
527 validate the outcomes of this research.

528 **5. Conclusions**

529 In our multiomics analysis of *GRINA* expression in cancer databases, we provide
530 evidence of a relationship between altered *GRINA* expression and clinical outcomes. Our
531 study reveals the significance of *GRINA* expression and possible *GRINA*-related molecular
532 mechanisms and pathways in cancer progression. The findings of this study thus may offer
533 valuable insights into the use of *GRINA* as a prospective therapeutic target for various
534 cancers.

535 **Abbreviations:** BLCA, bladder urothelial carcinoma; BRCA, invasive breast carcinoma;
536 CESC, Cervical squamous cell carcinoma; CHOL, cholangiocarcinoma; COAD, colon
537 adenocarcinoma; ESCA, esophageal carcinoma; GBM, glioblastoma
538 multiforme; HNSC, head and neck squamous cell carcinoma; KICH, kidney
539 chromophobe; KIRC, kidney renal clear cell carcinoma; KIRP, Kidney renal papillary cell
540 carcinoma; LIHC, Liver hepatocellular carcinoma; LUAD, Lung adenocarcinoma; LUSC,
541 Lung squamous cell carcinoma; PAAD, pancreatic adenocarcinoma; PRAD, Prostate
542 adenocarcinoma; PCPG, Pheochromocytoma and Paraganglioma; READ, rectum
543 adenocarcinoma; SARC, Sarcoma; SKCM, Skin Cutaneous Melanoma; THCA, thyroid
544 carcinoma; THYM, Thymoma; STAD, stomach adenocarcinoma; UCEC, uterine corpus
545 endometrial carcinoma; LAML, Acute Myeloid Leukemia; OV, Ovarian serous

546 cystadenocarcinoma; LBC, lobular breast cancer; IDBC, invasive ductal breast cancer;
547 HER2, human epidermal growth factor receptor 2; TNBC, triple-negative breast cancer; CC,
548 colon cancer; RADC, rectal adenocarcinomas; COAD, colon adenocarcinoma; MADC,
549 mucinous-adenocarcinoma; GM, Gastric Mucosa; GITA, Gastric Intestinal Type
550 Adenocarcinoma; GMA, Gastric Mixed Adenocarcinoma; STAD, stomach adenocarcinoma;
551 PG, Prostate Gland; PC, Prostate Carcinoma; PIN, Prostatic Intraepithelial Neoplasia; GS,
552 Gleason scores.

553 **Author Contributions:** Conceptualization, S.K.S.; methodology, S.K.S., and S.M.R.I.;
554 validation, S.K.S., and S.M.R.I.; formal analysis, S.K.S., S.M.R.I., S.E.-S., F.T., J.D., M.A.,
555 and S.-G.C; investigation, S.K.S., and S.M.R.I.; data curation, S.K.S., and S.M.R.I.; Funding
556 acquisition, S.-G.C.; writing—original draft preparation, S.M.R.I.; writing—review and
557 editing, S.K.S.; visualization, S.K.S.; supervision, S.K.S., and S.M.R.I. All authors have read
558 and agreed to the published version of the manuscript.

559 **Funding:** This study was supported by grants from the National Research Foundation (NRF)
560 funded by the Korean government (grant no. 2019M3A9H1030682 and
561 2015R1A5A1009701).

562 **Acknowledgments:** We are grateful to the contributors of data to Oncomine, UCSC Xena,
563 ULCAN, Human Protein Atlas, cBioPortal, R2: Kaplan Meier Scanner web, SurvExpress
564 web, miRSystem, starBase v3.0, InteractiVenn, Enrichr web, and Expression2Kinases (X2K)
565 web, which provides a Web resource for exploring, visualizing, and analyzing
566 multidimensional cancer genomics data.

Conflicts of Interest: The authors declare no conflict of interest. The funders had no role in the design of the study; in the collection, analyses, or interpretation of data; in the writing of the manuscript, or in the decision to publish the results.

References

[1] S.I. Deutsch, A.H. Tang, J.A. Burket, A.D. Benson, NMDA receptors on the surface of cancer cells: Target for chemotherapy?, Biomed Pharmacother, 68 (2014) 493-496.

[2] A. Stepulak, H. Luksch, C. Gebhardt, O. Uckermann, J. Marzahn, M. Sifringer, W. Rzeski, C. Staufner, K.S. Brocke, L. Turski, C. Ikonomidou, Expression of glutamate receptor subunits in human cancers, Histochem Cell Biol, 132 (2009) 435-445.

[3] W.G. North, G. Gao, A. Jensen, V.A. Memoli, J. Du, NMDA receptors are expressed by small-cell lung cancer and are potential targets for effective treatment, Clinical pharmacology : advances and applications, 2 (2010) 31-40.

[4] W.G. North, G. Gao, V.A. Memoli, R.H. Pang, L. Lynch, Breast cancer expresses functional NMDA receptors, Breast cancer research and treatment, 122 (2010) 307-314.

[5] W.K. Nahm, B.D. Philpot, M.M. Adams, E.V. Badiavas, L.H. Zhou, J. Butmarc, M.F. Bear, V. Falanga, Significance of N-methyl-d-aspartate (NMDA) receptor-mediated signaling in human keratinocytes, Journal of cellular physiology, 200 (2004) 309-317.

[6] H. Tamura, M. Suzuki, Y. Moriya, H. Hoshino, T. Okamoto, S. Yoshida, I. Yoshino, Aberrant methylation of N-methyl-D-aspartate receptor type 2B (NMDAR2B) in non-small cell carcinoma, BMC cancer, 11 (2011) 220.

[7] C. Collins, C. Duff, A.M.V. Duncan, R. Planellscases, W. Sun, A. Norremolle, E. Michaelis, M. Montal, R. Worton, M.R. Hayden, Mapping of the Human Nmda Receptor Subunit (Nmdar1) and the Proposed Nmda Receptor Glutamate-Binding Subunit (Nmdara1) to Chromosome-9q34.3 and Chromosome-8, Respectively, Genomics, 17 (1993) 237-239.

[8] W.G. North, F. Liu, R. Tian, H. Abbasi, B. Akerman, NMDA receptors are expressed in human ovarian cancer tissues and human ovarian cancer cell lines, Clin Pharmacol-Adv A, 7 (2015) 111-117.

[9] X. Gao, H.Y. Wang, S.B. Cai, M.R. Saadatzadeh, H. Hanenberg, K.E. Pollok, A.A. Cohen-Gadol, J.H. Chen, Phosphorylation of NMDA 2B at S1303 in human glioma peritumoral tissue: implications for glioma epileptogenesis, Neurosurg Focus, 37 (2014).

[10] K. Watanabe, T. Kanno, T. Oshima, H. Miwa, C. Tashiro, T. Nishizaki, The NMDA receptor NR2A subunit regulates proliferation of MKN45 human gastric cancer cells, Biochem Bioph Res Co, 367 (2008) 487-490.

[11] D. Rojas-Rivera, C. Hetz, TMBIM protein family: ancestral regulators of cell death, Oncogene, 34 (2015) 269-280.

[12] D. Rojas-Rivera, R. Armisen, A. Colombo, G. Martinez, A.L. Eguiguren, A. Diaz, S. Kiviluoto, D. Rodriguez, M. Patron, R. Rizzuto, G. Bultynck, M.L. Concha, J. Sierralta, A. Stutzin, C. Hetz, TMBIM3/GRINA is a novel unfolded protein response (UPR) target gene

605 that controls apoptosis through the modulation of ER calcium homeostasis, Cell Death Differ,
606 19 (2012) 1013-1026.

607 [13] D.H. Xu, Q. Li, H. Hu, B. Ni, X. Liu, C. Huang, Z.Z. Zhang, G. Zhao, Transmembrane
608 protein GRINA modulates aerobic glycolysis and promotes tumor progression in gastric
609 cancer, J Exp Clin Canc Res, 37 (2018).

610 [14] P. Habib, A.-S. Stamm, T. Zeyen, R. Noristani, A. Slowik, C. Beyer, T. Wilhelm, M.
611 Huber, D. Komnig, J.B. Schulz, EPO regulates neuroprotective Transmembrane BAX
612 Inhibitor-1 Motif-containing (TMBIM) family members GRINA and FAIM2 after cerebral
613 ischemia-reperfusion injury, Experimental neurology, 320 (2019) 112978.

614 [15] C. Connolly, S. Madden, D. Buggy, H. Gallagher, Expression of anaesthetic and
615 analgesic drug target genes in excised breast tumour tissue: Association with clinical disease
616 recurrence or metastasis, PloS one, 12 (2017) e0177105.

617 [16] D.B. Goswami, C.S. Jernigan, A. Chandran, A.H. Iyo, W.L. May, M.C. Austin, C.A.
618 Stockmeier, B. Karolewicz, Gene expression analysis of novel genes in the prefrontal cortex
619 of major depressive disorder subjects, Prog Neuro-Psychoph, 43 (2013) 126-133.

620 [17] H.-K. Kim, K.R. Bhattarai, R.P. Junjappa, J.H. Ahn, S.H. Pagire, H.J. Yoo, J. Han, D.
621 Lee, K.-W. Kim, H.-R. Kim, TMBIM6/BI-1 contributes to cancer progression through
622 assembly with mTORC2 and AKT activation, Nature communications, 11 (2020) 1-16.

623 [18] R.P. Junjappa, H.K. Kim, S.Y. Park, K.R. Bhattarai, K.W. Kim, J.W. Soh, H.R. Kim,
624 H.J. Chae, Expression of TMBIM6 in Cancers: The Involvement of Sp1 and PKC, Cancers,
625 11 (2019).

626 [19] K. Chen, X. Li, G. Song, T. Zhou, Y. Long, Q. Li, S. Zhong, Z. Cui, Deficiency in the
627 membrane protein Tmbim3a/Grinaa initiates cold-induced ER stress and cell death by
628 activating an intrinsic apoptotic pathway in zebrafish, J Biol Chem, 294 (2019) 11445-11457.

629 [20] D.R. Rhodes, S. Kalyana-Sundaram, V. Mahavisno, R. Varambally, J.J. Yu, B.B.
630 Briggs, T.R. Barrette, M.J. Anstet, C. Kincead-Beal, P. Kulkarni, S. Varambally, D. Ghoshy,
631 A.M. Chinnaiyan, Oncomine 3.0: Genes, pathways, and networks in a collection of 18,000
632 cancer gene expression profiles, Neoplasia, 9 (2007) 166-180.

633 [21] D.R. Rhodes, J.J. Yu, K. Shanker, N. Deshpande, R. Varambally, D. Ghosh, T. Barrette,
634 A. Pandey, A.M. Chinnaiyan, ONCOMINE: A cancer microarray database and integrated
635 data-mining platform, Neoplasia, 6 (2004) 1-6.

636 [22] S.K. Saha, Y. Jeong, S. Cho, S.G. Cho, Systematic expression alteration analysis of
637 master reprogramming factor OCT4 and its three pseudogenes in human cancer and their
638 prognostic outcomes, Sci Rep-Uk, 8 (2018).

639 [23] S.K. Saha, S.M.R. Islam, K.S. Kwak, M.S. Rahman, S.G. Cho, PROM1 and PROM2
640 expression differentially modulates clinical prognosis of cancer: a multiomics analysis,
641 Cancer gene therapy, (2019).

642 [24] M. Goldman, B. Craft, A. Brooks, J. Zhu, D. Haussler, The UCSC Xena Platform for
643 cancer genomics data visualization and interpretation, BioRxiv, (2018) 326470.

644 [25] D.S. Chandrashekar, B. Bashel, S.A.H. Balasubramanya, C.J. Creighton, I. Ponce-
645 Rodriguez, B. Chakravarthi, S. Varambally, UALCAN: A Portal for Facilitating Tumor
646 Subgroup Gene Expression and Survival Analyses, Neoplasia, 19 (2017) 649-658.

[26] S.K. Saha, Y. Yin, H.S. Chae, S.-G. Cho, Opposing Regulation of Cancer Properties via KRT19-Mediated Differential Modulation of Wnt/β-Catenin/Notch Signaling in Breast and Colon Cancers, Cancers, 11 (2019) 99.

[27] M. Uhlen, E. Bjorling, C. Agaton, C.A. Szigyarto, B. Amini, E. Andersen, A.C. Andersson, P. Angelidou, A. Asplund, C. Asplund, L. Berglund, K. Bergstrom, H. Brumer, D. Cerjan, M. Ekstrom, A. Elobeid, C. Eriksson, L. Fagerberg, R. Falk, J. Fall, M. Forsberg, M.G. Bjorklund, K. Gumbel, A. Halimi, I. Hallin, C. Hamsten, M. Hansson, M. Hedhammar, G. Hercules, C. Kampf, K. Larsson, M. Linskog, W. Lodewyckx, J. Lund, J. Lundeberg, K. Magnusson, E. Malm, P. Nilsson, J. Odling, P. Oksvold, I. Olsson, E. Oster, J. Ottosson, L. Paavilainen, A. Persson, R. Rimini, J. Rockberg, M. Runeson, A. Sivertsson, A. Skollermo, J. Steen, M. Stenvall, F. Sterky, S. Stromberg, M. Sundberg, H. Tegel, S. Tourle, E. Wahlund, A. Walden, J.H. Wan, H. Wernerus, J. Westberg, K. Wester, U. Wrethagen, L.L. Xu, S. Hober, F. Ponten, A human protein atlas for normal and cancer tissues based on antibody proteomics, Mol Cell Proteomics, 4 (2005) 1920-1932.

[28] M. Uhlen, L. Fagerberg, B.M. Hallstrom, C. Lindskog, P. Oksvold, A. Mardinoglu, A. Sivertsson, C. Kampf, E. Sjostedt, A. Asplund, I. Olsson, K. Edlund, E. Lundberg, S. Navani, C.A. Szigyarto, J. Odeberg, D. Djureinovic, J.O. Takanen, S. Hober, T. Alm, P.H. Edqvist, H. Berling, H. Tegel, J. Mulder, J. Rockberg, P. Nilsson, J.M. Schwenk, M. Hamsten, K. von Feilitzen, M. Forsberg, L. Persson, F. Johansson, M. Zwahlen, G. von Heijne, J. Nielsen, F. Ponten, Proteomics. Tissue-based map of the human proteome, Science, 347 (2015) 1260419.

[29] J.J. Gao, B.A. Aksoy, U. Dogrusoz, G. Dresdner, B. Gross, S.O. Sumer, Y.C. Sun, A. Jacobsen, R. Sinha, E. Larsson, E. Cerami, C. Sander, N. Schultz, Integrative Analysis of Complex Cancer Genomics and Clinical Profiles Using the cBioPortal, Sci Signal, 6 (2013).

[30] E. Cerami, J. Gao, U. Dogrusoz, B.E. Gross, S.O. Sumer, B.A. Aksoy, The cBio Cancer Genomics Portal: An Open Platform for Exploring Multidimensional Cancer Genomics Data (vol 2, pg 401, 2012), Cancer Discov, 2 (2012) 960-960.

[31] J. Koster, J.J. Molenaar, R. Versteeg, R2: Accessible web-based genomics analysis and visualization platform for biomedical researchers, Cancer Res, 75 (2015).

[32] R. Aguirre-Gamboa, H. Gomez-Rueda, E. Martinez-Ledesma, A. Martinez-Torteya, R. Chacolla-Huaringa, A. Rodriguez-Barrientos, J.G. Tamez-Pena, V. Trevino, SurvExpress: An Online Biomarker Validation Tool and Database for Cancer Gene Expression Data Using Survival Analysis, PloS one, 8 (2013).

[33] T.-P. Lu, C.-Y. Lee, M.-H. Tsai, Y.-C. Chiu, C.K. Hsiao, L.-C. Lai, E.Y. Chuang, miRSystem: an integrated system for characterizing enriched functions and pathways of microRNA targets, PloS one, 7 (2012) e42390.

[34] J.-H. Li, S. Liu, H. Zhou, L.-H. Qu, J.-H. Yang, starBase v2. 0: decoding miRNA-ceRNA, miRNA-ncRNA and protein–RNA interaction networks from large-scale CLIP-Seq data, Nucleic acids research, 42 (2013) D92-D97.

[35] J.C. Oliveros, VENNY. An interactive tool for comparing lists with Venn Diagrams. 2007, in, 2015.

[36] H. Heberle, G.V. Meirelles, F.R. da Silva, G.P. Telles, R. Minghim, InteractiVenn: a web-based tool for the analysis of sets through Venn diagrams, Bmc Bioinformatics, 16 (2015).

[37] E.Y. Chen, C.M. Tan, Y. Kou, Q.N. Duan, Z.C. Wang, G.V. Meirelles, N.R. Clark, A. Ma'ayan, Enrichr: interactive and collaborative HTML5 gene list enrichment analysis tool, Bmc Bioinformatics, 14 (2013).

[38] M.V. Kuleshov, M.R. Jones, A.D. Rouillard, N.F. Fernandez, Q.N. Duan, Z.C. Wang, S. Koplev, S.L. Jenkins, K.M. Jagodnik, A. Lachmann, M.G. McDermott, C.D. Monteiro, G.W. Gundersen, A. Ma'ayan, Enrichr: a comprehensive gene set enrichment analysis web server 2016 update, Nucleic acids research, 44 (2016) W90-W97.

[39] D.J.B. Clarke, M.V. Kuleshov, B.M. Schilder, D. Torre, M.E. Duffy, A.B. Keenan, A. Lachmann, A.S. Feldmann, G.W. Gundersen, M.C. Silverstein, Z.C. Wang, A. Ma'ayan, eXpression2Kinases (X2K) Web: linking expression signatures to upstream cell signaling networks, Nucleic acids research, 46 (2018) W171-W179.

[40] E.Y. Chen, H.L. Xu, S. Gordonov, M.P. Lim, M.H. Perkins, A. Ma'ayan, Expression2Kinases: mRNA profiling linked to multiple upstream regulatory layers, Bioinformatics, 28 (2012) 105-111.

[41] V. Jimenez-Gonzalez, E. Ogalla-Garcia, M. Garcia-Quintanilla, A. Garcia-Quintanilla, Deciphering GRINA/Lifeguard1: Nuclear Location, Ca2+ Homeostasis and Vesicle Transport, Int J Mol Sci, 20 (2019).

[42] L. Cheng, Q. Zhang, S. Yang, Y.Q. Yang, W. Zhang, H.J. Gao, X.X. Deng, Q.H. Zhang, A 4-gene panel as a marker at chromosome 8q in Asian gastric cancer patients, Genomics, 102 (2013) 323-330.

[43] L. Cheng, P. Wang, S. Yang, Y.Q. Yang, Q. Zhang, W. Zhang, H.S. Xiao, H.J. Gao, Q.H. Zhang, Identification of genes with a correlation between copy number and expression in gastric cancer, Bmc Med Genomics, 5 (2012).

[44] W.Y. Lou, J.X. Liu, B.S. Ding, L.Q. Jin, L. Xu, X. Li, J. Chen, W.M. Fan, Five miRNAs-mediated PIEZO2 downregulation, accompanied with activation of Hedgehog signaling pathway, predicts poor prognosis of breast cancer, Aging-Us, 11 (2019) 2628-2652.

[45] N. Sheng, Y.Z. Xu, Q.H. Xi, H.Y. Jiang, C.Y. Wang, Y. Zhang, Q. Ye, Overexpression of KIF2A is Suppressed by miR-206 and Associated with Poor Prognosis in Ovarian Cancer, Cell Physiol Biochem, 50 (2018) 810-822.

[46] N.A. Bowden, R.J. Scott, P.A. Tooney, Altered gene expression in the superior temporal gyrus in schizophrenia, Bmc Genomics, 9 (2008).

[47] A.K. Patel, V.D. Bhatt, A.K. Tripathi, M.R. Sajnani, S.J. Jakhesara, P.G. Koringa, C.G. Joshi, Identification of novel splice variants in horn cancer by RNA-Seq analysis in Zebu cattle, Genomics, 101 (2013) 57-63.

[48] T. Yamaji, K. Nishikawa, K. Hanada, Transmembrane BAX Inhibitor Motif Containing (TMBIM) Family Proteins Perturbs a trans-Golgi Network Enzyme, Gb3 Synthase, and Reduces Gb3 Biosynthesis, J Biol Chem, 285 (2010) 35505-35518.

[49] M. Grzmil, S. Kaulfuss, P. Thelen, B. Hemmerlein, S. Schweyer, S. Obenauer, T.W. Kang, P. Burfeind, Expression and functional analysis of Bax inhibitor-1 in human breast cancer cells, The Journal of pathology, 208 (2006) 340-349.

[50] D. Most, C. Leiter, Y.A. Blednov, R.A. Harris, R.D. Mayfield, Synaptic microRNAs Coordinately Regulate Synaptic mRNAs: Perturbation by Chronic Alcohol Consumption, Neuropsychopharmacol, 41 (2016) 538-548.

[51] C. Luna, G. Li, J. Qiu, D.L. Epstein, P. Gonzalez, MicroRNA-24 regulates the processing of latent TGFβ1 during cyclic mechanical stress in human trabecular meshwork cells through direct targeting of FURIN, Journal of cellular physiology, 226 (2011) 1407-1414.

[52] H. Urra, E. Dufey, F. Lisbona, D. Rojas-Rivera, C. Hetz, When ER stress reaches a dead end, Bba-Mol Cell Res, 1833 (2013) 3507-3517.

[53] R. van der Lee, M. Buljan, B. Lang, R.J. Weatheritt, G.W. Daughdrill, A.K. Dunker, M. Fuxreiter, J. Gough, J. Gsponer, D.T. Jones, P.M. Kim, R.W. Kriwacki, C.J. Oldfield, R.V. Pappu, P. Tompa, V.N. Uversky, P.E. Wright, M.M. Babu, Classification of Intrinsically Disordered Regions and Proteins, Chem Rev, 114 (2014) 6589-6631.

[54] M.E. Oates, P. Romero, T. Ishida, M. Ghalwash, M.J. Mizianty, B. Xue, Z. Dosztanyi, V.N. Uversky, Z. Obradovic, L. Kurgan, D2P2: database of disordered protein predictions, Nucleic acids research, 41 (2012) D508-D516.

[55] M. Ponente, L. Campanini, R. Cuttano, A. Piunti, G.A. Delledonne, N. Coltella, R. Valsecchi, A. Villa, U. Cavallaro, L. Pattini, C. Doglioni, R. Bernardi, PML promotes metastasis of triple-negative breast cancer through transcriptional regulation of HIF1A target genes, Jci Insight, 2 (2017).

[56] L. Arreal, M. Piva, S. Fernandez, A. Revandkar, A. Schaub-Clerigue, J. Villanueva, A. Zabala-Letona, M. Pujana, I. Astobiza, A.R. Cortazar, I. Hermanova, L. Bozal-Basterra, A. Arruabarrena-Aristorena, J.R. Crespo, L. Valcarcel-Jimenez, P. Zuniga-Garcia, F. Canals, V. Torrano, R. Barrio, J.D. Sutherland, A. Alimonti, N. Martin-Martin, A. Carracedo, Targeting PML in triple negative breast cancer elicits growth suppression and senescence, Cell Death Differ, (2019).

[57] S.E. Birch, J.G. Kench, E. Takano, P. Chan, A.L. Chan, K. Chiam, A.S. Veillard, P. Stricker, S. Haupt, Y. Haupt, L. Horvath, S.B. Fox, Expression of E6AP and PML predicts for prostate cancer progression and cancer-specific death, Annals of oncology : official journal of the European Society for Medical Oncology, 25 (2014) 2392-2397.

[58] H.J. Kim, D.E. Song, S.Y. Lim, S.H. Lee, J.L. Kang, S.J. Lee, E.N. Benveniste, Y.H. Choi, Loss of the promyelocytic leukemia protein in gastric cancer: implications for IP-10 expression and tumor-infiltrating lymphocytes, PloS one, 6 (2011) e26264.

[59] N. Datta, S. Islam, U. Chatterjee, S. Chatterjee, C.K. Panda, M.K. Ghosh, Promyelocytic Leukemia (PML) gene regulation: implication towards curbing oncogenesis, Cell death & disease, 10 (2019) 656.

[60] X. Cui, X. Jing, Q. Yi, C. Long, B. Tan, X. Li, X. Chen, Y. Huang, Z. Xiang, J. Tian, J. Zhu, Systematic analysis of gene expression alterations and clinical outcomes of STAT3 in cancer, Oncotarget, 9 (2018) 3198-3213.

[61] J.J. Qin, L. Yan, J. Zhang, W.D. Zhang, STAT3 as a potential therapeutic target in triple negative breast cancer: a systematic review, J Exp Clin Canc Res, 38 (2019).

Figure legends

Figure 1. A schematic diagram summarizing selected online tools used in this study.

Figure 2. *GRINA* (Glutamate Ionotropic Receptor NMDA Type Subunit Associated Protein 1) mRNA levels were analyzed in different types of cancer. (**a**) The mRNA expression of *GRINA* in various human cancers. The figure was retrieved from the Oncomine database. The cell number represents the dataset number that meets all the thresholds with the color blue for under-expression and color red for over-expression. Cell color is determined by the best gene rank percentile for the analyses within the cell. (**b**) The mRNA expression of *GRINA* in various human cancers. The figure was retrieved from the TCGA database using UCSC Xena. *p*-value < 0.05 represents statistically significant. *$p < 0.05$; ** $p < 0.01$; ***$p < 0.001$; ****$p < 0.0001$. (**c**) mRNA expression of *GRINA* was analyzed by RT-PCR using various cancer cell lines including breast (MCF7 and MDA-MB231), esophagus (SEG-1), colon (HCT116 and HT-29), liver (HepG2 and SNU475), blood (K562), lung (A549), and ovarian (SKOV3 and A2780), cancers. *GAPDH* was used as a loading control. The expression intensity of *GRINA* mRNA was analyzed by ImageJ software. The expression bands were cropped from the full gel with no apparent modification. The image of full gels is supplemented in supplementary information files under Supplementary Figure 1.

Figure 3. Expression of *GRINA* and patient survival were analysed in normal and cancerous breast tissue. (**a and b**) Fold-changes in *GRINA* levels in breast cancer, shown as box plots comparing *GRINA* expression in normal ($n = 3$, left plot) vs. lobular breast carcinoma tissue ($n = 21$, right plot) (**a**) and in normal ($n = 3$, left plot) vs. invasive ductal breast carcinoma tissue ($n = 38$, right plot) (**b**). Data derived from the Oncomine database. (**c**) *GRINA* mRNA levels were analyzed in breast cancer (n = 1097) and the normal (n = 114) tissues based on data from The Cancer Genome Atlas (TCGA) database using ULCAN web. (**d**) *GRINA* levels in BRCA patients (subclass) based on the TCGA database using ULCAN

web. (**e**) Methylation levels in *GRINA* promoters were analysed in breast cancer based on The Cancer Genome Atlas (TCGA) data and ULCAN. (**f**) Mutation and copy number alteration frequencies of *GRINA* were derived from cBioPortal using TCGA-BRCA data. (**g**) GRINA protein expression data from immunohistochemistry staining in normal and breast carcinomas was derived from the Human Protein Atlas. (**h**) Survival curves comparing breast cancer patients with high (red) and low (blue) *GRINA* levels based on the R2: Kaplan Meier Scanner (Pro) database. Survival curve analysis was conducted using a threshold logrank test using scan modus of expression value. p-value < 0.05 represents statistically significant.

Figure 4. *GRINA* expression patterns and patient survival analysis were performed for colorectal cancers. (**a and b**) Fold-changes in *GRINA* in colorectal cancers were identified by our analyses, shown as a box plot comparing *GRINA* levels in normal (n = 10, left plot) vs. colon carcinoma tissues (n = 5, right plot) (**a**) and normal (n = 65, left plot) vs. rectal adenocarcinoma tissue (n = 65, right plot) (**b**) based on data from the Oncomine database. (**c**) *GRINA* mRNA levels in colon adenocarcinoma were obtained from The Cancer Genome Atlas (TCGA) database through ULCAN. (**d**) *GRINA* expression in COAD patients (subclass) obtained from the TCGA database. (**e**) Methylation of *GRINA* gene promoters was analyzed in colon cancer based on data from The Cancer Genome Atlas (TCGA) database obtained via ULCAN. (**f**) Copy number alteration frequencies of the *GRINA* gene were derived from the cBioPortal web using TCGA-COAD data. (**g**) Protein expression of GRINA, as demonstrated by immunohistochemistry staining in normal tissue and colon carcinomas obtained from the Human Protein Atlas. (**h**) Survival curves for colon cancer patients with high (red) and low (blue) GRINA levels in colon cancer based on the R2:

822 Kaplan Meier Scanner (Pro) database. Survival curve analysis was conducted using a
823 threshold logrank test using scan modus of expression value. *p*-value < 0.05 represents
824 statistically significant.

825 **Figure 5.** *GRINA* expression patterns and patient survival were analysed in gastric cancers.
826 (**a and b**) Fold-changes of *GRINA* in gastric cancers is shown as box plots either comparing
827 *GRINA* levels in normal (*n* = 31, left plot) and gastric intestinal-type adenocarcinoma tissues
828 (*n* = 26, right plot) (**a**) or comparison normal (*n* = 31, left plot) and gastric mixed
829 adenocarcinoma tissues (*n* = 4, right plot) (**b**) based on the Oncomine database. (**c**)
830 *GRINA* mRNA levels in stomach carcinomas was obtained from The Cancer Genome Atlas
831 (TCGA) database through ULCAN. (**d**) *GRINA* gene expression in STAD patients (subclass)
832 was obtained from the TCGA database. (**e**) Methylation of *GRINA* gene promoters was
833 analyzed in STAD tumors (red plot) and normal (blue plot) tissues based on TCGA database
834 information and was generated using ULCAN. (**f**) Mutation and copy number alteration
835 frequencies of the *GRINA* gene were derived from the cBioPortal web using TCGA-STAD
836 data. (**g**) GRINA protein expression based on immunohistochemistry staining in normal and
837 stomach carcinoma tissues was derived from the Human Protein Atlas. (**h**) Survival curves
838 or stomach cancer patients were plotted with high (red) and low (blue) GRINA levels based
839 on the R2: Kaplan Meier Scanner (Pro) database. Survival curve analysis was conducted
840 using a threshold logrank test using scan modus of expression value. *p*-value < 0.05
841 represents statistically significant.

842 **Figure 6.** *GRINA* expression patterns and patient survival were analyzed for prostate cancer.
843 (**a and b**) The fold-changes in *GRINA* levels in prostate cancers are shown as box plots
844 comparing levels between normal (n = 23, left plot) and prostate carcinoma tissues (n = 30,
845 right plot) (**a**) and between normal (n = 23, left plot) and prostatic intraepithelial neoplasia
846 tissues (n = 13, right plot) (**b**) based on data derived from Oncomine. (**c**) *GRINA* mRNA
847 levels was analyzed in prostate adenocarcinomas from The Cancer Genome Atlas (TCGA)
848 database via ULCAN web. (**d**) *GRINA* expression levels was examined in PRAD patients
849 (Gleason score) from the TCGA database. (**e**) Methylation of *GRINA* gene was analyzed in
850 prostate cancer using The Cancer Genome Atlas (TCGA) database through the ULCAN web.
851 (**f**) Copy number alteration frequency of the *GRINA* gene was derived from the cBioPortal
852 web using TCGA-PRAD data. (**g**) Protein expression data for GRINA was obtained via
853 immunohistochemistry staining in normal and prostate carcinoma tissues from the Human
854 Protein Atlas. (**h**) Survival curves comparing patients with prostate cancer having high (red)
855 and low (blue) GRINA levels, plotted using data from the R2: Kaplan Meier Scanner (Pro)
856 database. Survival curve analysis was conducted using a threshold logrank test using scan
857 modus of expression value. p-value < 0.05 represents statistically significant.

858 **Figure 7.** Construction of a GRINA-miRNA-mRNA network. (**a**) GRINA mRNA-targeting
859 miRNAs were identified using miRSystem and starBase v3.0 databases. Common miRNAs
860 were identified using list of miRNAs derived from miRSystem and Starbase v3.0 via Venn
861 diagram. (**b**) A total of common 18 GRINA mRNA-targeting miRNAs were used to construct
862 the GRINA-miRNA-mRNA network using the starBase v3.0 database. (**c**) Expression of

863 miR-411-5p, miR-654-5p, and miR-874-3p was analysed in breast, colon, prostate, and
864 stomach cancer tissues and normal tissue controls as determined using starBase v3.0. (d)
865 Schematic of the in-silico analysis of the predicted binding sites showing that miR-411, miR-
866 654, and miR-874 bind to the 3′ UTR region of GRINA mRNA. The binding site of GRINA
867 3'UTR and miRNAs were derived from Starbase v3.0 web. The predicted consequential
868 pairing between the target region (position chr8; 145067249–145067271 of GRINA 3′ UTR)
869 and the seed sequence of miR-411 is shown (i). The predicted consequential pairing between
870 the target region (position chr8; 145067297–145067303 of GRINA 3′ UTR) and the seed
871 sequence of miR-654 is shown (ii). The predicted consequential pairing between the target
872 region (position chr8; 145067491–145067496 of GRINA 3′ UTR) and the seed sequence of
873 miR-874 is shown (iii). *p*-value < 0.05 represents statistically significant.

874 **Figure 8.** Pathway enrichment analysis for genes positively and negatively co-expressed
875 with GRINA in breast, colon, stomach, and prostate cancer. (**a**) Venn diagram of genes
876 positively co-expressed with GRINA based on R2: Genomics Analysis and Visualization
877 Platform databases for breast, colon, stomach, and prostate cancer, using InteractiVenn. (**b**
878 **and c**) Pathway (Reactome and KEGG) enrichment analysis was performed using Enrichr
879 for the 83 genes positively co-expressed with GRINA in breast, colon, stomach, and prostate
880 cancer. (**d**) The Venn diagram of genes negatively co-expressed with GRINA based on R2:
881 Genomics Analysis and Visualization Platform databases for breast, colon, stomach, and
882 prostate cancer using InteractiVenn web. (**e and f**) Pathway (KEGG and Reactome)

883 enrichment analysis was performed using Enrichr web for the 21 genes negatively co-
884 expressed with GRINA in breast, colon, stomach, and prostate cancer.

885 **Figure 9**. Subnetwork of transcription factors, intermediate proteins, and protein kinases.
886 Expression2Kinases analysis of the (**a**) positively- and (**b**) negatively co-expressed genes
887 indicated the most enriched TFs and kinase upstream of co-expressed genes occurring in
888 multiple cancers based on a combination of P-values and *z*-scores. Node size reflects
889 connectivity, and color indicates transcription factors in red, intermediate proteins in orange,
890 and kinases in blue.

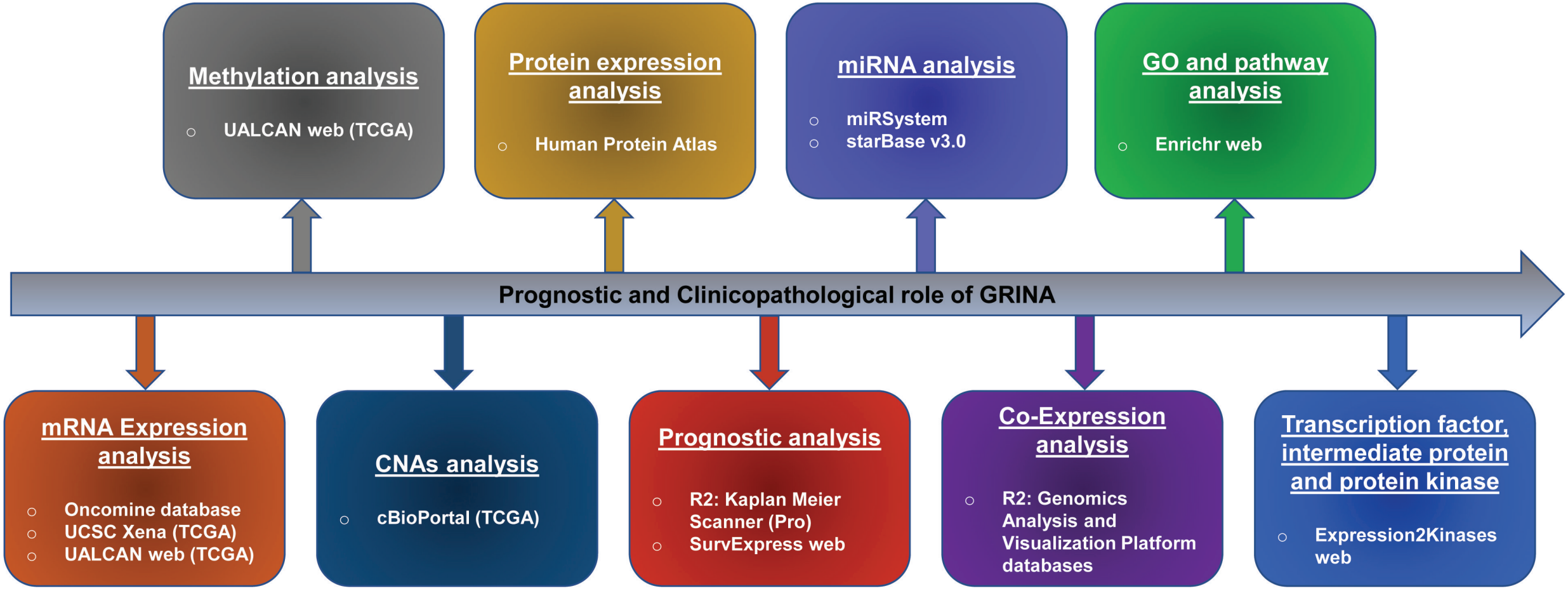
Methylation analysis
UALCAN web (TCGA)
Protein expression analysis
Human Protein Atlas
miRNA analysis
miRSystem
starBase v3.0
GO and pathway analysis
Enrichr web
Prognostic and Clinicopathological role of GRINA
mRNA Expression analysis
Oncomine database
UCSC Xena (TCGA)
UALCAN web (TCGA)
CNAs analysis
cBioPortal (TCGA)
Prognostic analysis
R2: Kaplan Meier Scanner (Pro)
SurvExpress web
Co-Expression analysis
R2: Genomics Analysis and Visualization Platform databases
Transcription factor, intermediate protein and protein kinase
Expression2Kinases web

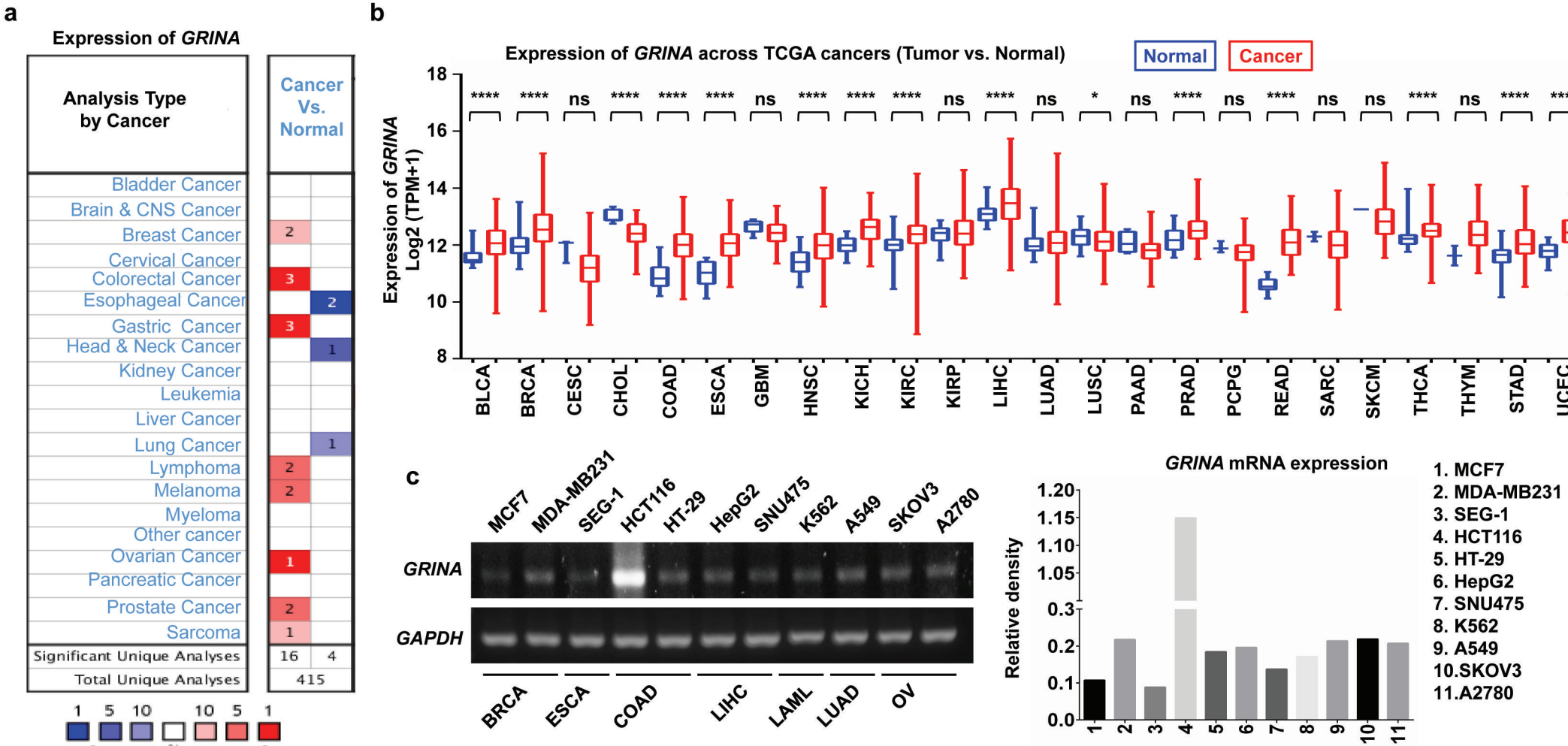
a
Expression of GRINA
Analysis Type by Cancer
Cancer Vs. Normal
Bladder Cancer
Brain & CNS Cancer
Breast Cancer
Cervical Cancer
Colorectal Cancer
Esophageal Cancer
Gastric Cancer
Head & Neck Cancer
Kidney Cancer
Leukemia
Liver Cancer
Lung Cancer
Lymphoma
Melanoma
Myeloma
Other cancer
Ovarian Cancer
Pancreatic Cancer
Prostate Cancer
Sarcoma
Significant Unique Analyses 16 4
Total Unique Analyses 415
1 5 10 10 5 1
%
Cell color is determined by the best gene rank percentile for the analyses within the cell.
NOTE: An analysis may be counted in more than one cancer type.
b
Expression of GRINA across TCGA cancers (Tumor vs. Normal)
Normal
Cancer
Expression of GRINA Log2 (TPM+1)
BLCA BRCA CESC CHOL COAD ESCA GBM HNSC KICH KIRC KIRP LIHC LUAD LUSC PAAD PRAD PCPG READ SARC SKCM THCA THYM STAD UCEC
c
MCF7 MDA-MB231 SEG-1 HCT116 HT-29 HepG2 SNU475 K562 A549 SKOV3 A2780
GRINA
GAPDH
BRCA ESCA COAD LIHC LAML LUAD OV
GRINA mRNA expression
Relative density
1. MCF7
2. MDA-MB231
3. SEG-1
4. HCT116
5. HT-29
6. HepG2
7. SNU475
8. K562
9. A549
10. SKOV3
11. A2780

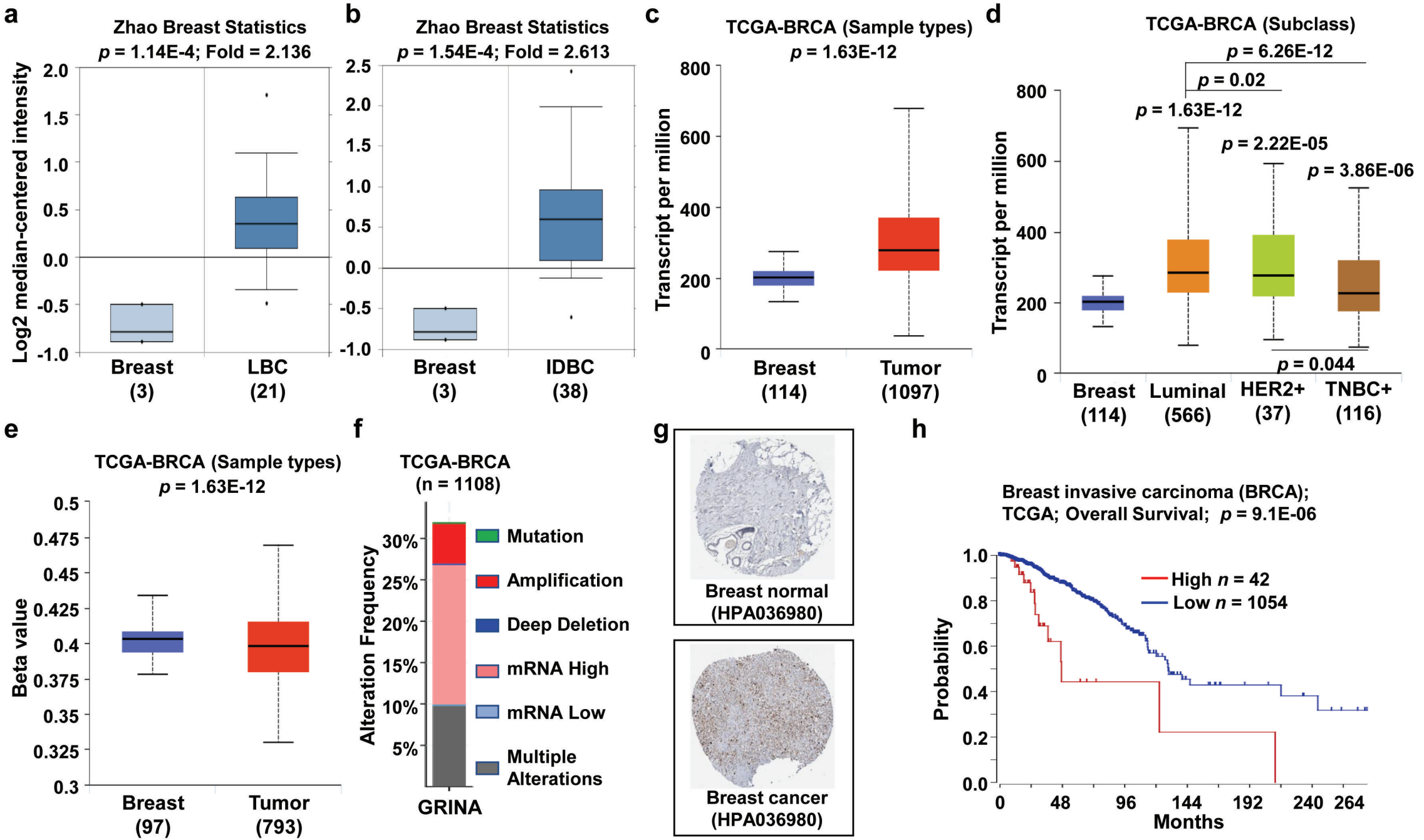
a
Zhao Breast Statistics
p = 1.14E-4; Fold = 2.136
Log2 median-centered intensity
2.0
1.5
1.0
0.5
0.0
-0.5
-1.0
Breast
(3)
LBC
(21)
b
Zhao Breast Statistics
p = 1.54E-4; Fold = 2.613
2.5
2.0
1.5
1.0
0.5
0.0
-0.5
-1.0
Breast
(3)
IDBC
(38)
c
TCGA-BRCA (Sample types)
p = 1.63E-12
Transcript per million
800
600
400
200
0
Breast
(114)
Tumor
(1097)
d
TCGA-BRCA (Subclass)
p = 6.26E-12
p = 0.02
p = 1.63E-12
p = 2.22E-05
p = 3.86E-06
p = 0.044
Transcript per million
800
600
400
200
0
Breast
(114)
Luminal
(566)
HER2+
(37)
TNBC+
(116)
e
TCGA-BRCA (Sample types)
p = 1.63E-12
Beta value
0.5
0.475
0.45
0.425
0.4
0.375
0.35
0.325
0.3
Breast
(97)
Tumor
(793)
f
TCGA-BRCA
(n = 1108)
Alteration Frequency
30%
25%
20%
15%
10%
5%
Mutation
Amplification
Deep Deletion
mRNA High
mRNA Low
Multiple
Alterations
GRINA
g
Breast normal
(HPA036980)
Breast cancer
(HPA036980)
h
Breast invasive carcinoma (BRCA);
TCGA; Overall Survival; p = 9.1E-06
High n = 42
Low n = 1054
Probability
1.0
0.8
0.6
0.4
0.2
0.0
0
48
96
144
192
240
264
Months

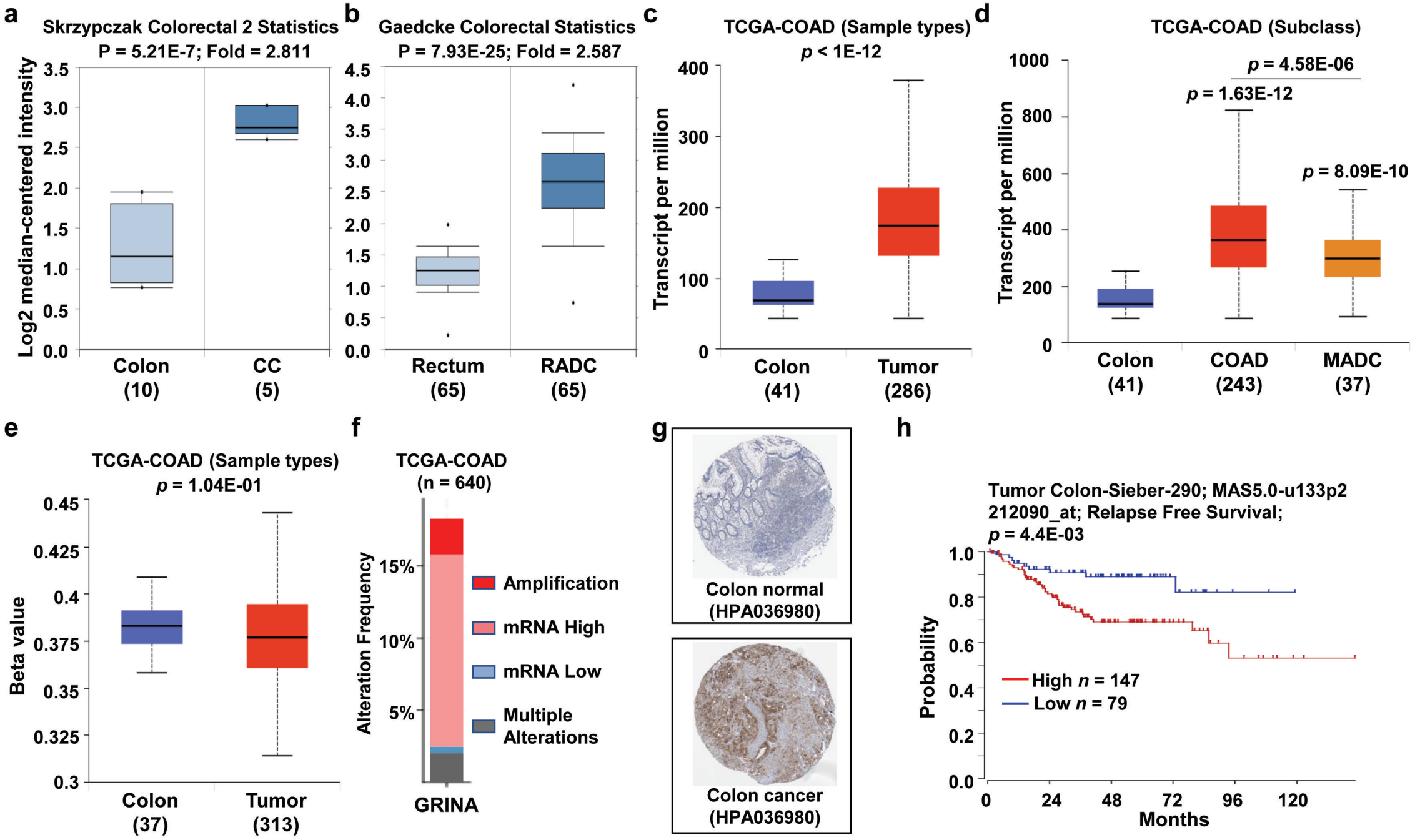
a
Skrzypczak Colorectal 2 Statistics
P = 5.21E-7; Fold = 2.811
Log2 median-centered intensity
3.5
3.0
2.5
2.0
1.5
1.0
0.5
0.0
Colon
(10)
CC
(5)
b
Gaedcke Colorectal Statistics
P = 7.93E-25; Fold = 2.587
4.5
4.0
3.5
3.0
2.5
2.0
1.5
1.0
0.5
0.0
Rectum
(65)
RADC
(65)
c
TCGA-COAD (Sample types)
p < 1E-12
Transcript per million
400
300
200
100
0
Colon
(41)
Tumor
(286)
d
TCGA-COAD (Subclass)
p = 4.58E-06
p = 1.63E-12
p = 8.09E-10
Transcript per million
1000
800
600
400
200
0
Colon
(41)
COAD
(243)
MADC
(37)
e
TCGA-COAD (Sample types)
p = 1.04E-01
Beta value
0.45
0.425
0.4
0.375
0.35
0.325
0.3
Colon
(37)
Tumor
(313)
f
TCGA-COAD
(n = 640)
Alteration Frequency
15%
10%
5%
Amplification
mRNA High
mRNA Low
Multiple
Alterations
GRINA
g
Colon normal
(HPA036980)
Colon cancer
(HPA036980)
h
Tumor Colon-Sieber-290; MAS5.0-u133p2
212090_at; Relapse Free Survival;
p = 4.4E-03
Probability
1.0
0.8
0.6
0.4
0.2
0.0
High n = 147
Low n = 79
0
24
48
72
96
120
Months

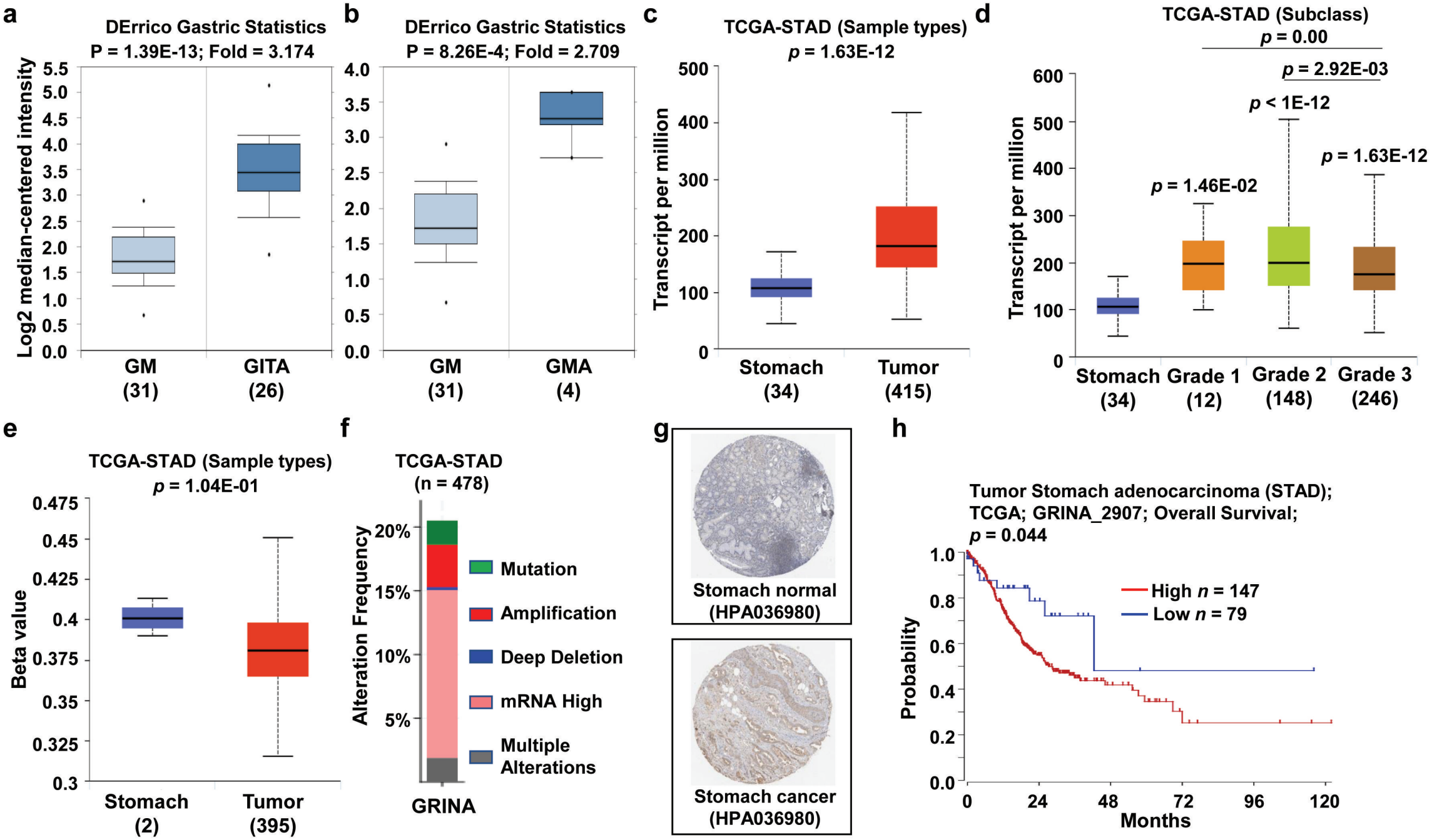
a
DErrico Gastric Statistics
P = 1.39E-13; Fold = 3.174
Log2 median-centered intensity
GM (31)
GITA (26)
b
DErrico Gastric Statistics
P = 8.26E-4; Fold = 2.709
GM (31)
GMA (4)
c
TCGA-STAD (Sample types)
p = 1.63E-12
Transcript per million
Stomach (34)
Tumor (415)
d
TCGA-STAD (Subclass)
p = 0.00
p = 2.92E-03
p < 1E-12
p = 1.63E-12
p = 1.46E-02
Transcript per million
Stomach (34)
Grade 1 (12)
Grade 2 (148)
Grade 3 (246)
e
TCGA-STAD (Sample types)
p = 1.04E-01
Beta value
Stomach (2)
Tumor (395)
f
TCGA-STAD
(n = 478)
Alteration Frequency
Mutation
Amplification
Deep Deletion
mRNA High
Multiple Alterations
GRINA
g
Stomach normal (HPA036980)
Stomach cancer (HPA036980)
h
Tumor Stomach adenocarcinoma (STAD);
TCGA; GRINA_2907; Overall Survival;
p = 0.044
High n = 147
Low n = 79
Probability
Months

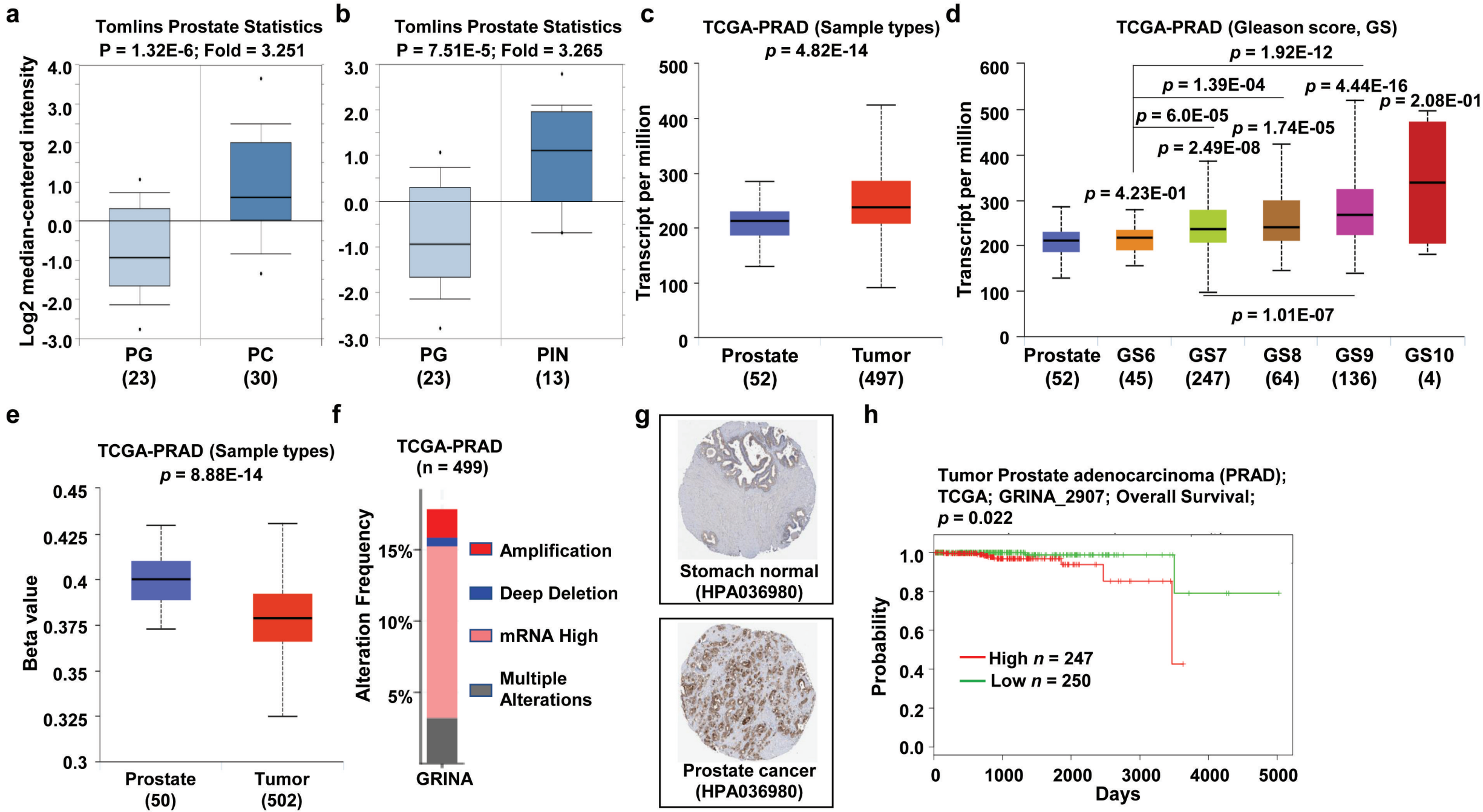
a
Tomlins Prostate Statistics
P = 1.32E-6; Fold = 3.251
Log2 median-centered intensity
4.0
3.0
2.0
1.0
0.0
-1.0
-2.0
-3.0
PG
(23)
PC
(30)
b
Tomlins Prostate Statistics
P = 7.51E-5; Fold = 3.265
3.0
2.0
1.0
0.0
-1.0
-2.0
-3.0
PG
(23)
PIN
(13)
c
TCGA-PRAD (Sample types)
p = 4.82E-14
Transcript per million
500
400
300
200
100
0
Prostate
(52)
Tumor
(497)
d
TCGA-PRAD (Gleason score, GS)
p = 1.92E-12
p = 1.39E-04
p = 4.44E-16
p = 6.0E-05
p = 1.74E-05
p = 2.08E-01
p = 2.49E-08
p = 4.23E-01
p = 1.01E-07
Transcript per million
600
500
400
300
200
100
0
Prostate
(52)
GS6
(45)
GS7
(247)
GS8
(64)
GS9
(136)
GS10
(4)
e
TCGA-PRAD (Sample types)
p = 8.88E-14
Beta value
0.45
0.425
0.4
0.375
0.35
0.325
0.3
Prostate
(50)
Tumor
(502)
f
TCGA-PRAD
(n = 499)
Alteration Frequency
15%
10%
5%
Amplification
Deep Deletion
mRNA High
Multiple
Alterations
GRINA
g
Stomach normal
(HPA036980)
Prostate cancer
(HPA036980)
h
Tumor Prostate adenocarcinoma (PRAD);
TCGA; GRINA_2907; Overall Survival;
p = 0.022
Probability
1.0
0.8
0.6
0.4
0.2
0.0
High n = 247
Low n = 250
0
1000
2000
3000
4000
5000
Days

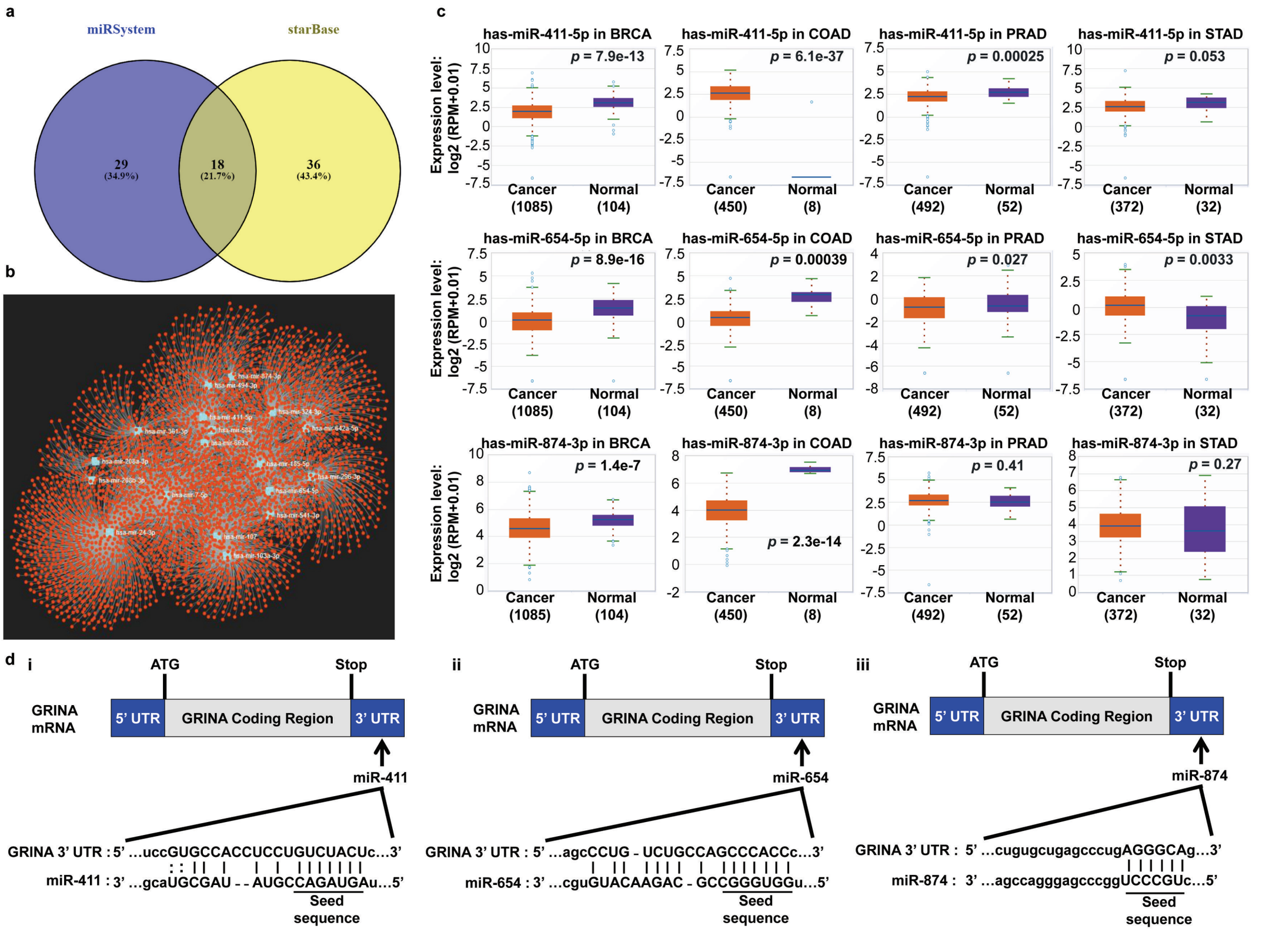
a
miRSystem
starBase
29
(34.9%)
18
(21.7%)
36
(43.4%)
b
hsa-mir-874-3p
hsa-mir-494-3p
hsa-mir-411-5p
hsa-mir-324-3p
hsa-mir-361-3p
hsa-mir-588
hsa-mir-642a-5p
hsa-mir-663a
hsa-mir-208a-3p
hsa-mir-185-5p
hsa-mir-208b-3p
hsa-mir-296-3p
hsa-mir-7-5p
hsa-mir-654-5p
hsa-mir-541-3p
hsa-mir-24-3p
hsa-mir-107
hsa-mir-103a-3p
c
has-miR-411-5p in BRCA
p = 7.9e-13
has-miR-411-5p in COAD
p = 6.1e-37
has-miR-411-5p in PRAD
p = 0.00025
has-miR-411-5p in STAD
p = 0.053
has-miR-654-5p in BRCA
p = 8.9e-16
has-miR-654-5p in COAD
p = 0.00039
has-miR-654-5p in PRAD
p = 0.027
has-miR-654-5p in STAD
p = 0.0033
has-miR-874-3p in BRCA
p = 1.4e-7
has-miR-874-3p in COAD
p = 2.3e-14
has-miR-874-3p in PRAD
p = 0.41
has-miR-874-3p in STAD
p = 0.27
Expression level: log2 (RPM+0.01)
Cancer (1085)
Normal (104)
Cancer (450)
Normal (8)
Cancer (492)
Normal (52)
Cancer (372)
Normal (32)
d
i
ii
iii
ATG
Stop
GRINA mRNA
5' UTR
GRINA Coding Region
3' UTR
miR-411
miR-654
miR-874
GRINA 3' UTR : 5' …uccGUGCCACCUCCUGUCUACUc…3'
miR-411 : 3' …gcaUGCGAU - - AUGCCAGAUGAu…5'
GRINA 3' UTR : 5' …agcCCUG - UCUGCCAGCCCACCc…3'
miR-654 : 3' …cguGUACAAGAC - GCCGGGUGGu…5'
GRINA 3' UTR : 5' …cugugcugagcccugAGGGCAg…3'
miR-874 : 3' …agccagggagcccggUCCCGUc…5'
Seed sequence

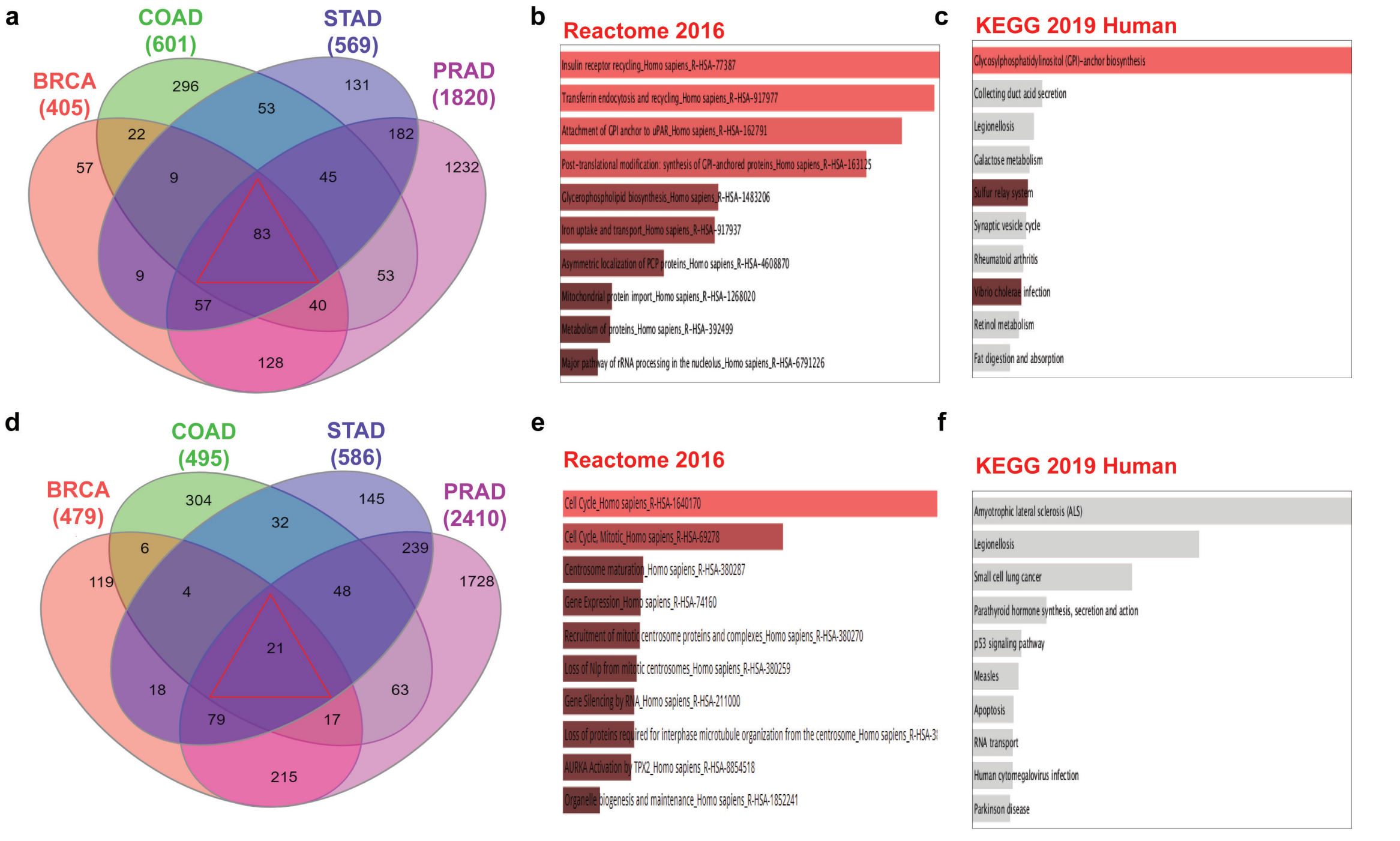
a
COAD
(601)
STAD
(569)
BRCA
(405)
PRAD
(1820)
296
131
53
22
182
57
9
45
1232
83
9
53
57
40
128
b
Reactome 2016
Insulin receptor recycling_Homo sapiens_R-HSA-77387
Transferrin endocytosis and recycling_Homo sapiens_R-HSA-917977
Attachment of GPI anchor to uPAR_Homo sapiens_R-HSA-162791
Post-translational modification: synthesis of GPI-anchored proteins_Homo sapiens_R-HSA-163125
Glycerophospholipid biosynthesis_Homo sapiens_R-HSA-1483206
Iron uptake and transport_Homo sapiens_R-HSA-917937
Asymmetric localization of PCP proteins_Homo sapiens_R-HSA-4608870
Mitochondrial protein import_Homo sapiens_R-HSA-1268020
Metabolism of proteins_Homo sapiens_R-HSA-392499
Major pathway of rRNA processing in the nucleolus_Homo sapiens_R-HSA-6791226
c
KEGG 2019 Human
Glycosylphosphatidylinositol (GPI)-anchor biosynthesis
Collecting duct acid secretion
Legionellosis
Galactose metabolism
Sulfur relay system
Synaptic vesicle cycle
Rheumatoid arthritis
Vibrio cholerae infection
Retinol metabolism
Fat digestion and absorption
d
COAD
(495)
STAD
(586)
BRCA
(479)
PRAD
(2410)
304
145
32
6
239
119
4
48
1728
21
18
63
79
17
215
e
Reactome 2016
Cell Cycle_Homo sapiens_R-HSA-1640170
Cell Cycle, Mitotic_Homo sapiens_R-HSA-69278
Centrosome maturation_Homo sapiens_R-HSA-380287
Gene Expression_Homo sapiens_R-HSA-74160
Recruitment of mitotic centrosome proteins and complexes_Homo sapiens_R-HSA-380270
Loss of Nlp from mitotic centrosomes_Homo sapiens_R-HSA-380259
Gene Silencing by RNA_Homo sapiens_R-HSA-211000
Loss of proteins required for interphase microtubule organization from the centrosome_Homo sapiens_R-HSA-3
AURKA Activation by TPX2_Homo sapiens_R-HSA-8854518
Organelle biogenesis and maintenance_Homo sapiens_R-HSA-1852241
f
KEGG 2019 Human
Amyotrophic lateral sclerosis (ALS)
Legionellosis
Small cell lung cancer
Parathyroid hormone synthesis, secretion and action
p53 signaling pathway
Measles
Apoptosis
RNA transport
Human cytomegalovirus infection
Parkinson disease

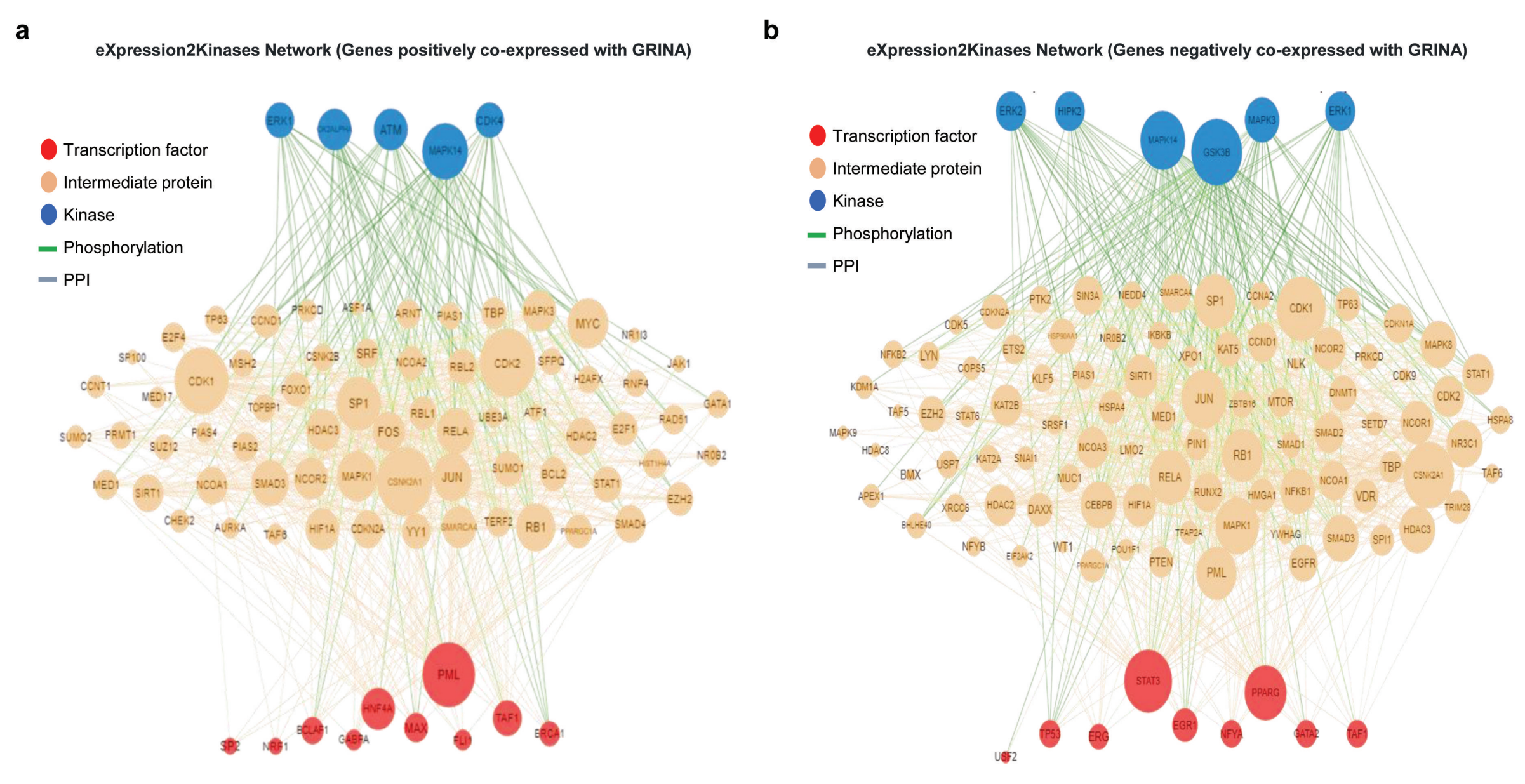
a
eXpression2Kinases Network (Genes positively co-expressed with GRINA)
Transcription factor
Intermediate protein
Kinase
Phosphorylation
PPI
ERK1
ATM
MAPK14
CDK4
TP63
CCND1
PRKCD
ASF1A
ARNT
PIAS1
TBP
MAPK3
MYC
NR1I3
E2F4
SF100
MSH2
CSNK2B
SRF
NCOA2
RBL2
CDK2
SFPQ
JAK1
CCNT1
CDK1
MED17
FOXO1
H2AFX
RNF4
TOPBP1
SP1
RBL1
UBE3A
ATF1
GATA1
SUMO2
PRMT1
PIAS4
HDAC3
FOS
RELA
HDAC2
E2F1
RAD51
SUZ12
PIAS2
HIST1H4A
NR0B2
MED1
SIRT1
NCOA1
SMAD3
NCOR2
MAPK1
CSNK2A1
JUN
SUMO1
BCL2
STAT1
EZH2
CHEK2
AURKA
TAF8
HIF1A
CDKN2A
YY1
SMARCA4
TERF2
RB1
PPARGC1A
SMAD4
PML
HNF4A
MAX
TAF1
BCLAF1
GABPA
FLI1
BRCA1
SP2
NRF1
b
eXpression2Kinases Network (Genes negatively co-expressed with GRINA)
Transcription factor
Intermediate protein
Kinase
Phosphorylation
PPI
ERK2
HIPK2
MAPK14
GSK3B
MAPK3
ERK1
PTK2
SIN3A
NEDD4
SMARCA4
SP1
CCNA2
CDK1
TP63
CDKN2A
CDK5
CDKN1A
NFKB2
LYN
ETS2
HSP90AA1
NR0B2
IKBKB
XPO1
KAT5
CCND1
NCOR2
MAPK8
COPS5
KLF5
PIAS1
SIRT1
NLK
PRKCD
CDK9
STAT1
KDM1A
JUN
ZBTB16
MTOR
DNMT1
CDK2
TAF5
EZH2
STAT6
KAT2B
HSPA4
MED1
SETD7
NCOR1
HSPA8
MAPK9
SRSF1
SMAD2
NR3C1
HDAC8
NCOA3
LMO2
PIN1
SMAD1
RB1
TBP
BMX
USP7
KAT2A
SNAI1
RELA
CSNK2A1
TAF6
MUC1
NCOA1
APEX1
RUNX2
HMGA1
NFKB1
VDR
XRCC6
HDAC2
DAXX
CEBPB
HIF1A
TRIM28
BHLHE40
MAPK1
NFYB
WT1
TFAP2A
YWHAG
SMAD3
SPI1
HDAC3
EIF2AK2
POU1F1
PPARGC1A
PTEN
PML
EGFR
STAT3
PPARG
TP53
ERG
EGR1
NFYA
GATA2
TAF1
USF2

Supplementary Information

Expression of GRINA Correlates with Prognosis in Human Cancers: A Pan-cancer Analysis

S. M. Riazul Islam [1, †], Subbroto Kumar Saha [2, 3, †, *], Shaker El-Sappagh [4], Faisal Tariq [5], Joydeep Das [6], Muhammad Afzal [7], and Ssang-Goo Cho [2, *]

[1] Department of Computer Science and Engineering, Sejong University, 209 Neungdong-ro, Gwangjin-gu, Seoul, 05006, Republic of Korea; riaz@sejong.ac.kr (S.M.R.I)
[2] Department of Stem Cell and Regenerative Biotechnology, Konkuk University, 120 Neungdong-Ro, Seoul 05029, Republic of Korea; subbroto@konkuk.ac.kr (S.K.S.).
[3] Department of Biochemistry and Molecular Medicine, University of California at Davis, School of Medicine, Sacramento, California 95817, USA
[4] Centro Singular de Investigación en Tecnoloxías Intelixentes (CiTIUS), Universidade de Santiago de Compostela, 15782, Santiago de Compostela, Spain; shaker.elsappagh@usc.es (S.E.S.)
[5] James Watt School of Engineering, University of Glasgow, Glasgow G12 8QQ, United Kingdom; Faisal.Tariq@glasgow.ac.uk (F.T.)
[6] School of Chemistry, Shoolini University of Biotechnology and Management Sciences, Bajhol, Sultanpur, Solan – 173229 (HP), India; jdchem83@gmail.com (J.D.)
[7] Department of Software, Sejong University, Seoul 05006, South Korea; mafzal@sejong.ac.kr (M.A.)
***** Correspondence: sksaha@ucdavis.edu (S.K.S.); ssangoo@konkuk.ac.kr (S.-G.C.); Tel.: +1 (410) 413-0532 (S.K.S.); Tel.: +82-2-450-4207 (S.-G.C.); Fax: +82-2-444-4207 (S.-G.C.)
[†] These authors contributed equally to this work: S.M.R. Islam and S.K. Saha (co-first authors).

Supplementary Table 1. Changes in GRINA expression at the transcriptional level between different types of cancer and normal tissues (Oncomine Database).

Cancer type	Dataset	Normal (Cases)	Tumour (Cases)	Fold change	t-Test	p-value	Rank (%)	Reporter	PMID	GEO Accession
Breast	Zhao	Breast (3)	Lobular Breast Carcinoma (21)	2.136	6.534	1.14E-04	7	IMAGE: 769933 (2)	15034139	GSE3971
		Breast (3)	Invasive Ductal Breast Carcinoma (38)	2.613	8.179	1.54E-05	7	IMAGE: 769933 (2)	15034139	GSE3971
Colorectal	Hong	Colon (12)	Colorectal Carcinoma (70)	3.761	17.027	1.96E-18	1	212090_at	20143136	GSE9348
	Gaedcke	Rectum (65)	Rectal Adenocarcinoma (65)	2.587	14.11	7.93E-25	3	A_23_P316960	20725992	GSE20842
	Skrzypczak 2	Colon (10)	Colon Carcinoma (5)	2.811	8.939	5.21E-07	8	212090_at	20957034	GSE20916
Esophagus	Hao	Esophagus (11)	Esophageal Adenocarcinoma (2)	-5.61	-11.584	1.64E-11	1	IMAGE: 954354	16952561	GSE6059
		Esophagus (11)	Barrett's Esophagus (12)	-3.168	-2.902	6.00E-03	4	IMAGE: 954354	16952561	GSE6059
Gastric	DErrico	Gastric Mucosa (31)	Gastric Intestinal Type Adenocarcinoma (26)	3.174	10.113	1.39E-13	1	212090_at	19081245	GSE13911
		Gastric Mucosa (31)	Gastric Mixed Adenocarcinoma (4)	2.709	6.66	8.26E-04	9	212090_at	19081245	GSE13911
	Chen	Gastric Mucosa (24)	Gastric Mixed Adenocarcinoma (8)	2.244	4.923	1.80E-04	4	IMAGE: 953791	12925757	N/A
	Cho	Gastric Tissue (19)	Gastrointestinal Stromal Tumour (6)	2.884	6.774	1.65E-04	6	ILMN_2370872	21447720	GSE13861
Head and Neck	Cromer	Uvula (4)	Head and Neck Squamous Cell Carcinoma (34)	-2.009	-6.183	1.90E-06	2	32505_at	14676830	GSE2379
Lung	Garber	Lung (5)	Squamous Cell Lung Carcinoma (12)	-2.398	-4.113	7.31E-04	8	IMAGE: 769933	11707590	GSE3398
Lymphoma	Compagno	Germinal Center B-Lymphocyte (10)	Activated B-Cell-Like Diffuse Large B-Cell Lymphoma (17)	2.127	7.796	4.36E-09	5	212090_at	19412164	GSE12195
	Piccaluga	CD4-Positive T-Lymphocyte (5)	Angioimmunoblastic T-Cell Lymphoma (6)	2.052	7.02	4.91E-05	9	212090_at	17304354	GSE6338
Melanoma	Haqq	Skin (3)	Non-Neoplastic Nevus (9)	2.3	6.789	2.80E-05	3	AA455271	15833814	N/A
	Talantov	Skin (7)	Cutaneous Melanoma (45)	3.423	10.429	2.14E-06	5	212090_at	16243793	GSE3189
Ovarian	Bonome	Ovarian Surface Epithelium (10)	Ovarian Carcinoma (185)	4.354	25.6	4.85E-21	1	212090_at	18593951	GSE26712
Prostate	Tomlins	Prostate Gland (23)	Prostate Carcinoma (30)	3.251	5.296	1.32E-06	2	IMAGE: 810038	17173048	GSE6099
		Prostate Gland (23)	Prostatic Intraepithelial Neoplasia (13)	3.265	4.476	7.51E-05	3	IMAGE: 810038	17173048	GSE6099

Supplementary Table 2. Changes in GRINA expression at the transcriptional level between different types of cancer and normal tissues (TCGA Database).

Order	Cancer type	# of normal samples	# of cancer samples	GRINA expression in cancer (High/Low)	p-value (Welch's t-test)
1	Bladder urothelial carcinoma (BLCA)	19	408	High	5.4E-06
2	Breast invasive carcinoma (BRCA)	114	1097	High	4.6E-38
3	Cervical squamous cell carcinoma (CESC)	3	305	Low	0.3771
4	Cholangiocarcinoma (CHOL)	9	36	Low	3.05E-06
5	Colon adenocarcinoma (COAD)	4	286	High	2.25E-22
6	Esophageal carcinoma (ESCA)	11	184	High	4.81E-06
7	Glioblastoma multiforme (GBM)	5	156	Low	0.289002
8	Head and neck squamous cell carcinoma (HNSC)	44	520	High	1.52E-10
9	Kidney chromophobe (KICH)	25	67	High	2.42E-09
8	Kidney renal clear cell carcinoma (KIRC)	72	533	High	1.28E-12
11	Kidney renal papillary cell carcinoma (KIRP)	32	290	Low	0.386717
12	Liver hepatocellular carcinoma (LIHC)	50	371	High	4.65E-10
13	Lung adenocarcinoma (LUAD)	59	515	High	0.278277
14	Lung squamous cell carcinoma (LUSC)	52	503	Low	0.014681
15	Pancreatic adenocarcinoma (PAAD)	4	178	Low	0.432492
16	Prostate adenocarcinoma (PRAD)	52	497	High	5.12E-10
17	Pheochromocytoma and Paraganglioma (PCPG)	3	179	Low	0.240684
18	Rectum adenocarcinoma (READ)	10	166	High	7.18E-14

19	Sarcoma (SARC)	2	260	Low	N/A
20	Skin Cutaneous Melanoma (SKCM)	1	472	Low	N/A
21	Thyroid carcinoma (THCA)	59	505	High	9.3E-15
22	Thymoma (THYM)	2	120	High	N/A
23	Stomach adenocarcinoma (STAD)	34	415	High	7E-09
24	Uterine corpus endometrial carcinoma (UCEC)	35	546	High	6.1E-12

Supplementary Table 3. Transcription factors regulating genes positively and negatively co-expressed with GRINA identified using Expression2Kinases (X2K).

Rank	Transcription factor	Hypergeometric P-value	Z-score	Combined score	# of Enriched targets	Enriched targets
Transcription factors as positive co-expressed genes of GRINA						
1	GABPA	2.16E-08	0	0	31	ERGIC3 ALG3 FBXL6 TSNARE1 SHARPIN C8ORF33 C8ORF82 NFS1 ZNF7 CPSF1 C20ORF24 EIF6 NSUN5 ZNF696 NDUFB9 ZNF707 COMMD5 EXOSC4 SCAND1 SLC52A2 DDX56 RPL8 ACOT8 GLI4 GPS1 MAF1 ZFP41 ZNF517 PUF60 ADRM1 ROMO1
2	PML	8.28E-08	0	0	26	DGAT1 FBXL6 SHARPIN EEF1D SCRIB VPS28 ZC3H3 ZNF7 CHRAC1 CPSF1 DYNLRB1 MFSD3 NSUN5 NDUFB9 EXOSC4 SCAND1 CYC1 SLC52A2 PPDPF C16ORF13 RPL8 TIGD5 MAF1 STIP1 PUF60 ADRM1
3	SP2	0.00005086	0	0	16	EIF6 ZNF696 RHPN1-AS1 ZNF707 COMMD5 SHARPIN ATP6AP1 ACOT8 GLI4 MAF1 STIP1 ZNF517 ADRM1 ZNF7 DYNLRB1 CYHR1
4	MAX	0.001836	0	0	21	G6PC3 ALG3 BOP1 EEF1D ADCK5 CHRAC1 CPSF1 PYCRL MFSD3 PIGU NSUN5 NDUFB9 HSF1 SCAND1 DDX56 CLCN7 TIGD5 PUF60 PTDSS2 PTDSS1 SPNS1
5	HNF4A	0.006105	0	0	14	EIF6 NSUN5 ZNF696 DGAT1 TMEM150A SCAND1 SHARPIN DDX56 VPS28 MAF1 SLC39A4 C8ORF59 MAFG-AS1 CHRAC1
6	TAF1	0.009444	0	0	27	DGAT1 G6PC3 EEF1D C8ORF33 ADCK5 CHRAC1 CPSF1 NSUN5 SCAND1 CYC1 STIP1 ZNF517 PUF60 SPNS1 ALG3 SHARPIN TRAPPC9 PIGU PSMA7 NDUFB9 EXOSC4 TIMM17B RPL8 ACOT8 TIGD5 MAF1 PTDSS1
7	BCLAF1	0.01318	0	0	10	EXOSC4 SCAND1 SHARPIN SCRIB GLI4 MAF1 C8ORF33 ZNF7 CPSF1 MFSD3
8	NRF1	0.01618	0	0	17	ERGIC3 EEF1D VPS28 MAFG-AS1 TRAPPC9 ZC3H3 ADCK5 CPSF1 DYNLRB1 C20ORF24 NELFCD GPAA1 SCAND1 CCDC167 DDX56 TIGD5 ATP6V1F

9	FLI1	0.02038	0	0	8	SCRIB NSUN5 C8ORF82 NDUFB9 FBXL6 EXOSC4 SLC52A2 DDX56
10	BRCA1	0.02048	0	0	25	G6PC3 EEF1D ZC3H3 ADCK5 CHRAC1 CPSF1 MFSD3 ZNF696 SCAND1 BCAP31 CYC1 C16ORF13 PUF60 SPNS1 ATP6V1F CYHR1 C20ORF24 PSMA7 THEM6 NDUFB9 EXOSC4 TIMM17B DDX56 TIGD5 PTDSS1
Transcription factors as negative co-expressed genes of GRINA						
1	ERG	0.01343	0	0	2	CEP192 RANBP2
2	STAT3	0.01974	0	0	2	CHD9 AKAP13
3	PPARG	0.02628	0	0	3	RANBP2 CHD9 MCPH1
4	USF2	0.02722	0	0	4	PCM1 KLHL28 BTBD7 RANBP2
5	SIX5	0.04059	0	0	4	ZNF45 WRN PCM1 KLHL28
6	NFYA	0.04617	0	0	6	WRN CEP192 AKAP13 TNRC6B DICER1 MIER1
7	EGR1	0.0562	0	0	2	PCM1 TNRC6B
8	STAT3	0.05636	0	0	3	APAF1 TNRC6B KLHL28
9	TP53	0.05747	0	0	2	CHD9 APAF1
10	GATA2	0.0656	0	0	3	CHD9 TNRC6B MCPH1

Supplementary Table 4. Protein kinases likely acting on genes positively- and negatively co-expressed with GRINA that are responsible for phosphorylation of PPI in various cancers.

Rank	Protein kinase	Hypergeometric P-value	Z-score	Combined score	# of Enriched Substrates	Enriched Substrates
Protein kinases associated with genes positively co-expressed with GRINA						
1	CSNK2A1	1.45E-25	0	0	53	ATF1 CSNK2A1 PPARGC1A JUN EZH2 FOS SIRT1 STAT1 YY1 PIAS1 MSH2 MAX FOXO1 SUMO1 SUMO2 ARNT SRF E2F1 CSNK2B SMARCA4 BRCA1 NCOA2 RELA UBE3A CCND1 SFPQ AURKA RB1 MYC MED1 HIF1A TERF2 NCOR2 BCLAF1 CDKN2A CDK2 BCL2 CDK1 HDAC2 HDAC3 PML RAD51 CHEK2 GABPA PRMT1 SUZ12 SMAD4 SMAD3 TOPBP1 H2AFX RBL2 RBL1 MAPK1
2	CDK1	1.09E-19	0	0	49	CSNK2A1 PPARGC1A JUN EZH2 FOS SIRT1 STAT1 CCNT1 MSH2 NRF1 FOXO1 SP2 SP1 E2F1 E2F4 CSNK2B SMARCA4 BRCA1 HNF4A NCOA2 RELA UBE3A CCND1 SFPQ AURKA TAF1 RB1 MYC MED1 HIF1A NCOR2 BCLAF1 CDKN2A CDK2 BCL2 CDK1 HDAC2 PML RAD51 CHEK2 SUZ12 SMAD4 SMAD3 TOPBP1 H2AFX RBL2 RBL1 MAPK1 MAPK3
3	MAPK14	7.22E-16	0	0	35	PPARGC1A JUN EZH2 FOS STAT1 YY1 MSH2 FOXO1 SP1 E2F1 CSNK2B SMARCA4 BRCA1 HNF4A NCOA2 RELA CCND1 AURKA RB1 MYC HIF1A TERF2 NCOR2 BCLAF1 CDKN2A CDK2 BCL2 CDK1 RAD51 SUZ12 SMAD4 SMAD3 TOPBP1 RBL2 MAPK1
4	CDK2	3.23E-15	0	0	52	JUN MED17 FOS MSH2 SP2 SP1 E2F1 E2F4 TP63 CSNK2B SMARCA4 UBE3A RNF4 TERF2 NCOR2 CDKN2A BCL2 HDAC2 PML GABPA TOPBP1 H2AFX RBL2 RBL1 MAPK1 EZH2 STAT1 CCNT1 YY1 FOXO1 SUMO1 SUMO2 BRCA1 NCOA2 CCND1 SFPQ AURKA TAF6 TAF1 RB1 MYC MED1 HIF1A BCLAF1 CDK2

						CDK1 RAD51 CHEK2 PRMT1 SUZ12 SMAD4 SMAD3
5	MAPK1	6.11E-15	0	0	30	RB1 MYC MED1 CSNK2A1 GATA1 HIF1A JUN NR0B2 EZH2 FOS TERF2 NCOR2 BCLAF1 CDKN2A STAT1 FOXO1 SP1 CDK2 BCL2 CDK1 PML BRCA1 NCOA1 NCOA2 RELA CCND1 SMAD4 SMAD3 RBL2 MAPK1
6	CK2ALPHA	1.65E-14	0	0	21	ATF1 RB1 MYC CSNK2B JUN SMARCA4 BRCA1 NCOR2 RELA UBE3A YY1 MAX SP1 CDK1 SUMO1 ARNT HDAC2 HDAC3 SRF PML TAF1
7	ATM	2.83E-13	0	0	20	RB1 CHEK2 TP63 MED1 HIF1A SMARCA4 EZH2 BRCA1 TERF2 BCLAF1 MSH2 SP1 CDK2 CDK1 TOPBP1 H2AFX RBL2 RBL1 E2F1 RAD51
8	CDK4	8.52E-12	0	0	15	RB1 CCND1 MYC MAX FOXO1 JUN SMAD3 SP1 CDK2 BCL2 BRCA1 SUMO1 RBL2 RBL1 CDKN2A
9	MAPK3	1.59E-11	0	0	20	MYC MED1 GATA1 JUN NR0B2 NCOA1 NCOA2 FOS STAT1 CCND1 FOXO1 SMAD4 SMAD3 SP1 CDK2 BCL2 CDK1 E2F4 MAPK3 PML
10	ERK1	8.37E-11	0	0	15	MYC PRKCD GATA1 HIF1A JUN SMAD4 SMAD3 SP1 BCL2 JAK1 FOS NCOR2 SRF RELA STAT1

Protein kinase associated with genes negatively co-expressed with GRINA

1	CSNK2A1	4.26E-24	0	0	58	SPI1 DAXX CSNK2A1 PPARGC1A JUN EZH2 SIRT1 PPARG EGFR STAT1 STAT3 APEX1 PIAS1 PIN1 PTEN HSP90AA1 SRSF1 TRIM28 TP53 EGR1 XRCC6 SMARCA4 NCOA3 RELA CCND1 TFAP2A VDR HMGA1 BHLHE40 YWHAG CCNA2 RB1 MED1 HIF1A SNAI1 CDKN1A NCOR2 NCOR1 CDKN2A USP7 DNMT1 COPS5 CDK5 CDK2 CDK1 SIN3A CEBPB HDAC2 HDAC3 MTOR PML XPO1 KDM1A HSPA8 SMAD3 HSPA4 MAPK9 MAPK1
2	MAPK1	5.62E-21	0	0	40	RB1 MED1 CSNK2A1 HIF1A LYN JUN EIF2AK2 NR0B2 SNAI1 EZH2 CDKN1A NCOR2 PPARG EGFR CDKN2A STAT1 STAT3 ERG SP1 CDK2 CDK1 PTEN CEBPB PML RUNX2 TP53 EGR1 PTK2 NCOA1 RELA NR3C1 ETS2 CCND1 SMAD2 SMAD1 SMAD3 HMGA1 BHLHE40

						MAPK8 MAPK1
3	MAPK14	2.42E-18	0	0	42	PPARGC1A JUN EIF2AK2 EZH2 EGFR STAT1 STAT3 APEX1 SP1 PTEN HSP90AA1 SRSF1 TP53 EGR1 SMARCA4 NCOA3 RELA NR3C1 CCND1 HMGA1 BHLHE40 CCNA2 RB1 HIF1A CDKN1A NCOR2 NCOR1 CDKN2A DNMT1 CDK5 CDK2 CDK1 SIN3A CEBPB KAT5 RUNX2 XPO1 HSPA8 SMAD3 MAPK8 MUC1 MAPK1
4	CDK1	5.10E-17	0	0	52	CSNK2A1 GATA2 PPARGC1A LYN JUN EZH2 SIRT1 EGFR STAT1 STAT3 APEX1 NFKB1 SP1 PTEN HSP90AA1 SRSF1 TRIM28 TP53 EGR1 SMARCA4 NCOA3 RELA CCND1 HMGA1 BHLHE40 YWHAG CCNA2 TAF1 RB1 MED1 HIF1A CDKN1A NCOR2 NCOR1 CDKN2A USP7 DNMT1 CDK2 CDK1 SIN3A CEBPB HDAC2 MTOR PML KAT5 RUNX2 XPO1 NFYA KDM1A SMAD3 MAPK8 MAPK1
5	ERK1	8.61E-17	0	0	22	ETS2 KAT5 PRKCD RUNX2 TP53 HIF1A LYN SMAD2 SMAD1 JUN SMAD3 NFKB1 PTK2 SP1 NCOR2 CEBPB EGFR RELA MAPK8 STAT1 STAT3 MTOR
6	ERK2	4.44E-16	0	0	21	RB1 ETS2 RUNX2 TP53 SMAD2 SMAD1 JUN SMAD3 NFKB1 PTK2 SP1 NCOA1 NCOA3 NCOR2 PPARG CEBPB EGFR RELA STAT1 STAT3 MTOR
7	GSK3B	3.27E-15	0	0	55	GATA2 JUN PPARG EGFR PIAS1 SP1 PTEN TP63 TP53 EGR1 PTK2 SMARCA4 RELA NR3C1 BHLHE40 USF2 SNAI1 CDKN1A NCOR2 NCOR1 CDKN2A CEBPB MTOR PML KAT5 KDM1A MAPK8 MUC1 MAPK1 DAXX LYN EZH2 SIRT1 STAT1 STAT3 NFKB1 NFKB2 NCOA3 CCND1 HMGA1 CCNA2 TAF1 RB1 MED1 HIF1A DNMT1 CDK2 CDK1 SIN3A KLF5 RUNX2 SMAD2 HSPA8 SMAD1 SMAD3
8	MAPK3	3.55E-15	0	0	26	MED1 RUNX2 TP53 EGR1 JUN NR0B2 PTK2 CDKN1A NCOA1 PPARG EGFR STAT1 STAT3 NR3C1 ETS2 CCND1 SMAD2 SMAD3 SP1 BHLHE40 CDK2 CDK1

						PTEN CEBPB MAPK8 PML
9	MAPK8	6.73E-15	0	0	23	RUNX2 TP53 EGR1 JUN CDKN1A NCOA3 SIRT1 PPARG EGFR STAT6 CDKN2A STAT1 STAT3 NR3C1 CCND1 TFAP2A HMGA1 SP1 BHLHE40 CDK1 PTEN SIN3A MAPK1
10	HIPK2	1.29E-13	0	0	18	TRIM28 TP63 TP53 HIF1A SMAD2 SMAD1 XRCC6 SMAD3 HMGA1 NFKB1 IKBKB SIN3A SIRT1 NCOR1 CEBPB RELA MAPK8 PML

Supplementary Figure 1. Agarose gel picture of GRINA and GAPDH. Numbers indicate the cell lines added in Figure 2. Arrows indicate the size of PCR product.

Supplementary Figure 2. *GRINA* mRNA expression analysis in different cancer types (TCGA database). *GRINA* expression levels from data in the Cancer Genome Atlas (TCGA) database. Box plots showing *GRINA* mRNA levels in various tumours and corresponding normal tissues derived from data in TCGA database through ULCAN. (Abbreviations: BLCA-bladder urothelial carcinoma; CESC-cervical squamous cell carcinoma and endocervical adenocarcinoma; CHOL-cholangial carcinoma; ESCA-oesophageal carcinoma; GBM-glioblastoma multiforme; HNSC-head and neck squamous cell carcinoma; KIRC-kidney renal clear cell carcinoma; LIHC-liver hepatocellular carcinoma; LUAD-lung adenocarcinoma; PAAD-pancreatic adenocarcinoma; READ-rectum adenocarcinoma; SARC-sarcoma; THYM-thymoma; THCA-thyroid carcinoma; UCEC-uterine corpus endometrial carcinoma).

Supplementary Figure 3. Prognostic relevance of GRINA mRNA levels in various cancers based on TCGA data and SurvExpress (Available at http://bioinformatica.mty.itesm.mx:8080/Biomatec/SurvivaX.jsp). Survival curve analysis with a threshold of cox P-value < 0.05.

Supplementary Figure 4. GO functional annotation analysis for genes positively and negatively co-expressed with GRINA in breast, colon, stomach, and prostate cancer. (**a-c**) GO functional annotation (biological process, molecular function, and cellular component) was performed using Enrichr for 83 genes positively co-expressed with GRINA in breast, colon, stomach, and prostate cancer. (**d-f**) GO functional annotation (biological process, molecular function, and cellular component) was performed using Enrichr web for the 21 genes negatively co-expressed with GRINA in breast, colon, stomach, and prostate cancer.

Supplementary Figure 1

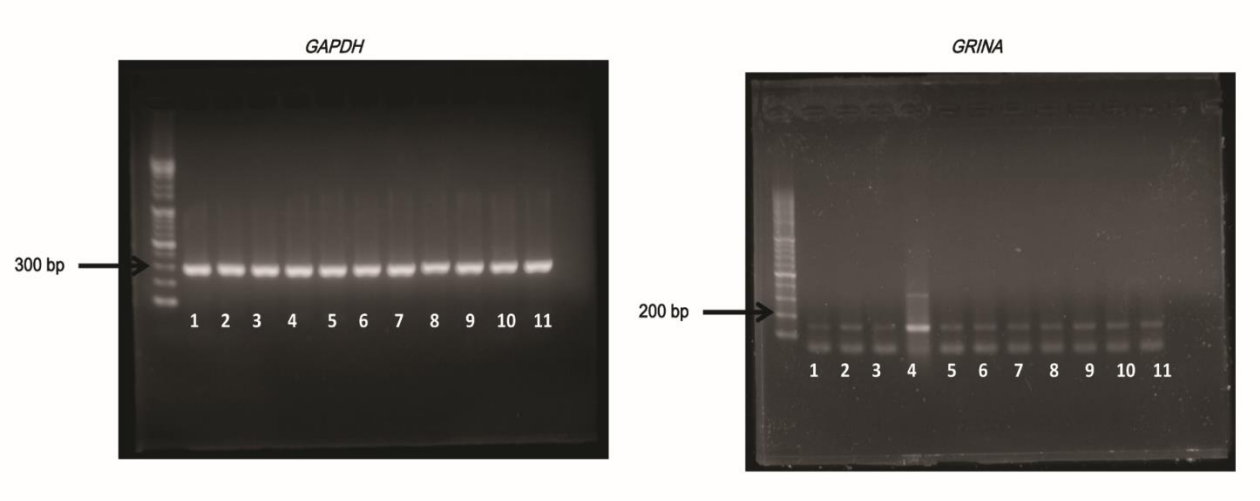

Supplementary Figure 2

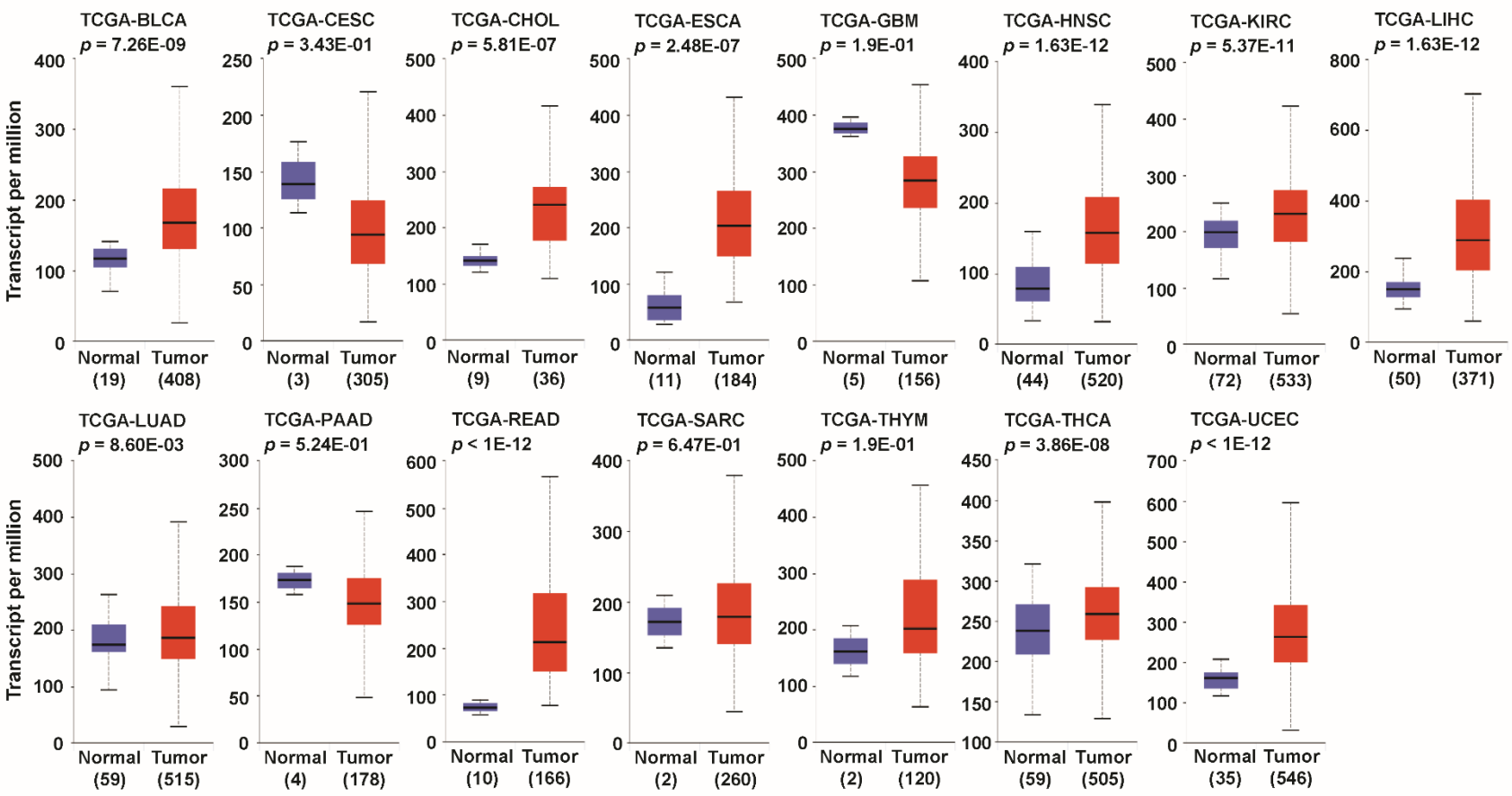

Supplementary Figure 3

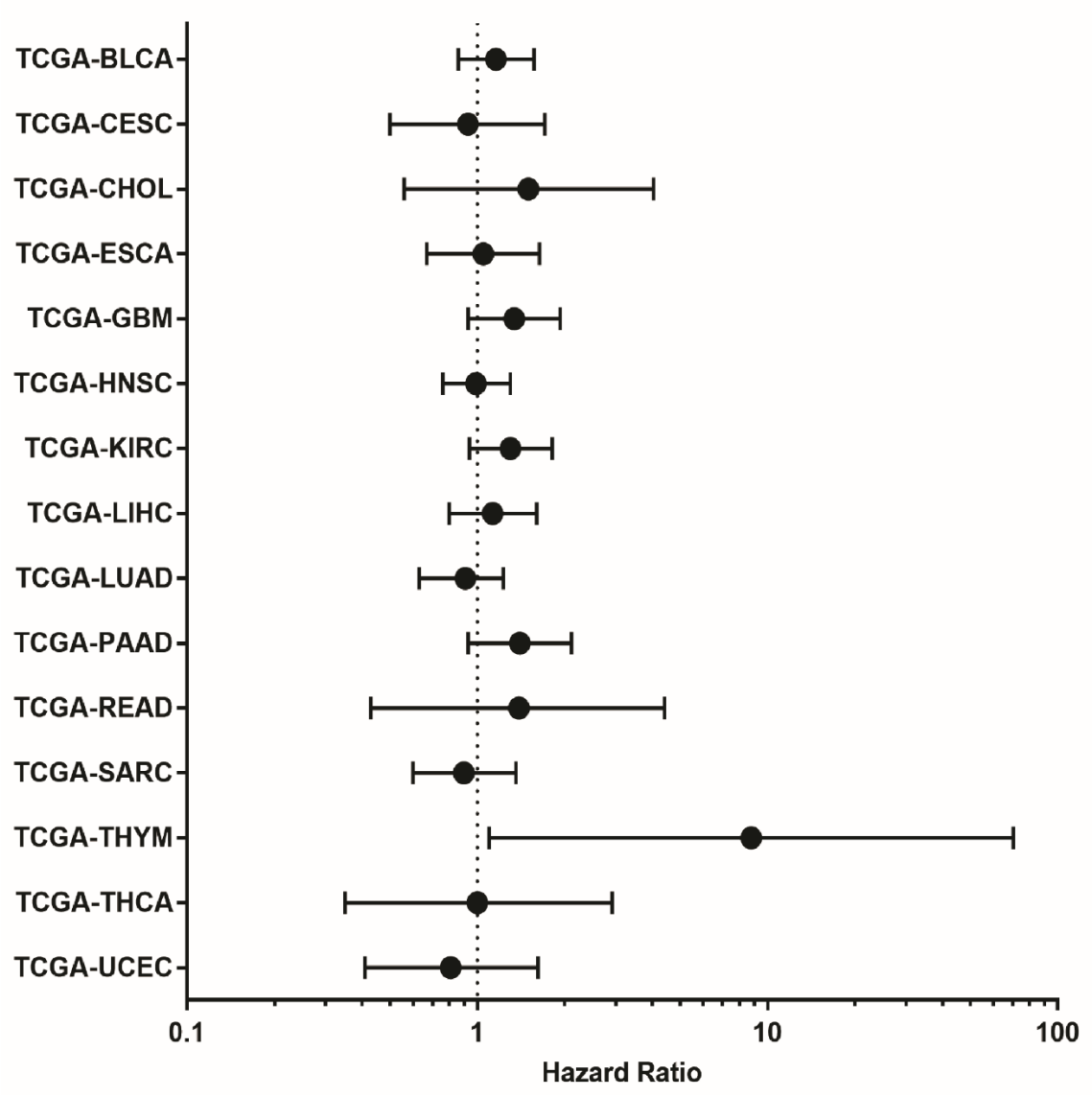

Supplementary Figure 4